AN INVESTIGATION ON PLASMA ANTENNAS

A THESIS SUBMITTED TO
THE GRADUATE SCHOOL OF NATURAL AND APPLIED SCIENCES
OF
MIDDLE EAST TECHNICAL UNIVERSITY

BY

RECEP FIRAT TİĞREK

IN PARTIAL FULFILLMENT OF THE REQUIREMENTS
FOR
THE DEGREE OF MASTER OF SCIENCE
IN
ELECTRICAL AND ELECTRONICS ENGINEERING

AUGUST 2005

Approval of the Graduate School of Natural and Applied Sciences

_____

Prof. Dr. Canan ÖZGEN

Director

I certify that this thesis satisfies all the requirements as a thesis for the degree of Master of Science.

_____

Prof. Dr. İsmet ERKMEN

Head of Department

This is to certify that we have read this thesis and that in our opinion it is fully adequate, in scope and quality, as a thesis for the degree of Master of Science.

_____

Prof. Dr. Altunkan HIZAL

Supervisor

Examining Committee Members

Prof. Dr. Canan TOKER (METU, EE)   _____

Prof. Dr. Altunkan HIZAL (METU, EE)   _____

Prof. Dr. Sinan BİLİKMEN (METU, PHYS)   _____

Assoc. Prof. Dr. Sencer KOÇ (METU, EE)   _____

Erhan HALAVUT M.S.E.E. (ASELSAN)   _____

I hereby declare that all information in this document has been obtained and presented in accordance with academic rules and ethical conduct. I also declare that, as required by these rules and conduct, I have fully cited and referenced all material and results that are not original to this work.

Name, Last name: Recep Fırat TİĞREK

Signature   :

ABSTRACT

AN INVESTIGATION ON PLASMA ANTENNAS

TİĞREK, Recep Fırat

M.S., Department of Electrical and Electronics Engineering

Supervisor: Prof. Dr. Altunkan HIZAL

August 2005, 79 pages

The plasma antennas offer a new solution to new requirements that are imposed on antenna systems with the advancing communication technology and increasing demand on wider frequency bands. In this thesis the plasma antennas are investigated for the radar and communication applications. The interaction of gas and semiconductor plasma with electromagnetic waves is inspected theoretically, and several experiments on the interaction of microwaves with gas plasma are conducted. Results of these experiments show that a relatively simple setup can produce plasma dense enough to interact with microwaves of frequency about 8 GHz. The previous studies of other institutes on plasma antennas are surveyed, emphasizing the results important for the use in radar and communication applications. Finally, semiconductor plasma is introduced, and an antenna system utilizing the semiconductor plasma generated by optical excitation is proposed.

ÖZ

PLAZMA ANTENLERİ ÜZERİNE BİR İNCELEME

TİĞREK, Recep Fırat

Yüksek Lisans, Elektrik ve Elektronik Mühendisliği Bölümü

Tez Yöneticisi: Prof. Dr. Altunkan HIZAL

Ağustos 2005, 79 sayfa

Plazma antenleri, gelişen iletişim teknolojisinin ve daha geniş frekans bantları için yükselen talebin anten sistemlerine yüklediği ek gerekleri karşılamak için yeni bir çözüm olarak ortaya çıkmıştır. Bu tezde plazma antenleri, radar ve iletişim alanındaki uygulamalar açısından ele alınmıştır. Gaz ve yarıiletken plazmanın elektromanyetik dalgalarla etkileşimi teorik olarak incelenmiş ve gaz plazma ile mikro dalga etkileşimi üzerine bazı deneyler yapılmıştır. Deneylerin sonuçları, 8 GHz frekanstaki mikro dalga ile etkileşimde bulunmaya yetecek yoğunlukta plazmanın nispeten basit bir düzenekle elde edilebildiğini göstermektedir. Plazma antenleri üzerine geçmişte diğer enstitüler tarafından yapılan çalışmalar, radar ve iletişim uygulamaları açısından önemli olan sonuçlar vurgulanarak incelenmiştir. En son olarak yarıiletken plazma tanıtılmış ve optik uyarılma ile oluşturulan yarıiletken plazmanın kullanıldığı bir anten sistemi önerilmiştir.

Anahtar kelimeler: Plazma antenleri, plazma frekansı, DC plazma, plazma yansıtıcı, yarıiletken plazma

To my family

and

in the memory of Prof. Dr. Ordal DEMOKAN

ACKNOWLEDGEMENTS

The author would like to express his gratitude to his advisor, Prof. Dr. Altunkan HIZAL, for his guidance and patience throughout this thesis. His critiques and advices enriched the content of the thesis and taught the author much about systematically approaching to a research project. Without his support and supervision, the thesis could not be completed.

The experimental apparatus was prepared by Prof. Dr. Ordal DEMOKAN, who passed away unexpectedly on 29.10.2004, in a car accident. His enthusiasm, knowledge and positive personality are deeply missed. The author would like to thank him for all he has done and could do.

The author would like to express his gratitude and thanks to his family for their continuous support, helpful discussions and advices. Without the help and skill of his father, Mr. Atilla TİĞREK, the experimental apparatus could never function.

Especially during the experimental stage, a great amount of time had to be diverted from the work hours to experiments. The author thanks ASELSAN Inc. for the permission to study on the thesis by departing in work hours. Also thanks goes to the colleagues in Test Engineering for their support.

For her encouraging when he stumble, her listening patiently, and her helping greatly in the drawings of the thesis, the author would like to express his gratitude to his fiancée, Müge TANYER.

TABLE OF CONTENTS

LIST OF FIGURES

FIGURES

CHAPTER 1

INTRODUCTION

Applications of plasma find wider use in our technology everyday. From huge and sophisticated projects of fusion to material processing to simple lighting equipment, the plasma research is one of the most generously funded research topics. On many of the plasma applications, the plasma is generated, heated or manipulated by RF radiation.

The plasma is a state of matter in which charged particles such as electrons and atom nuclei have sufficiently high energy to move freely, rather than be bound in atoms as in ordinary matter. Some examples of plasma are the fluorescent lighting tubes, lightning, and ionosphere. The plasma state can also be reached in crystalline structures. Semiconductor materials have electrons in the conduction band and holes in the valance band that move freely. The behavior of charge carriers in semiconductor crystalline structures is analogous to the behavior of particles in gas plasma.

Since the plasma consists of free charge carriers it is a conductor of electricity, and interaction of particles in plasma is governed by the laws of electromagnetism and thermodynamics.

Being a conductor of electricity, plasma is a reconfigurable medium with different conductor and dielectric properties. Plasma offers many solutions for the increasing need for reconfigurable and ultra wideband antenna systems by different generation and manipulation techniques and a wide range of electrical parameters. The generation techniques depend on the intended use; DC discharges, RF discharges and laser excitation are the most frequently used ones in gas plasma generation. Semiconductor plasma can be generated by optical excitation or current injection. The gas plasma is usually manipulated by magnetic fields; gas plasma can be confined in magnetic fields to prevent loss of energy to collision with vessel walls.

1.1. RESEARCH AIMS

The aims of this thesis are:

- To investigate the interaction of plasma and electromagnetic radiation

- To implement a basic plasma experimentation setup that will demonstrate the interaction of plasma and electromagnetic waves

- To gain the know-how required for the studies on applications of plasma for the use in radar antennas

- To propose a plasma antenna for the future studies.

1.2. RESEARCH OBJECTIVES

To realize the research aims, the research objectives that must be completed are:

- To derive the equations that govern the interaction of plasma and electromagnetic waves

- To find the relationship between the physical properties and the electrical characteristics of gas plasma

- To perform a literature survey on the plasma antennas

- To construct an experimental setup that generates gas plasma

- To conduct experiments on the interaction of plasma and microwaves and make comments on the results considering to the expected outcome according to the mathematical derivations

- To analyze the noise performance and dispersive nature of the plasma medium for the radar antenna applications

- To investigate semiconductor plasma.

1.3.   GUIDE TO THESIS

In order to understand why a plasma antenna concept has arisen, the equations governing the interaction of plasma and electromagnetic waves are derived in Chapter 2. The derivation starts from the behavior of a single charged particle under the influence of a plane electromagnetic wave. Then the discussion is carried on to the behavior of plasma by relating the particle behavior to current density. Effects of electron-neutral collision and static magnetic fields are also considered.

The plasma generation technique available for experimentation was DC discharge. The basic characteristics of DC discharge plasmas are given in Chapter 3. The electrical control of plasma properties is essential to reconfigure the plasma antennas, so the equations that bind the current density to plasma properties are derived as well.

In Chapter 4, the setup that generates the plasma is inspected. The components required for the generation of plasma with specific properties are introduced with circuit diagrams. The microwave experiments and their results are also given, and comments are made upon the results.

The plasma antenna concept is not new, however a worldwide interest on the subject has arisen in the last 15 years. Especially during the last years, the interest has shifted towards the military and commercial uses of the plasma antennas. Several application concepts and studies on these applications are inspected in Chapter 5. The radiation temperature of plasma reflector configuration is formulated. Also the dispersive nature of plasma medium is graphically demonstrated. Semiconductor plasma is explained and introduced in the last part of Chapter 5.

An antenna array structure that employs the semiconductor plasma is proposed in Chapter 6. In the system, semiconductor plasma will be generated by optical excitation. The feasibility of the proposed system is theoretically shown; optical power required for the antenna application is calculated for pure silicon as the semiconductor material.

It must be noted that, unless stated otherwise, the plasma mentioned throughout the thesis refers to gas plasma.

CHAPTER 2

INTERACTION OF PLASMA MEDIUM WITH ELECTROMAGNETIC WAVES

2.1. INTRODUCTION

Various materials are used within many antenna systems for different purposes today. The fundamental parts of an antenna structure are conducting parts, which guide and radiate the electromagnetic waves. Dielectric materials find an ever growing use in antenna structures.

The possibility of using the plasma medium in antenna structures arises from the electrical properties of the plasma medium. The electrical properties of a medium that are important in applications of electromagnetics are the conductivity, electrical permittivity and magnetic permeability. With these parameters known, propagation of electromagnetic waves in plasma medium can be inspected thoroughly.

Since ions and electrons are the constituents of plasma medium, interaction of electromagnetic waves with the plasma medium can be formulated by starting from the behavior of a single charged particle under the effect of an electromagnetic wave.

2.2. CONDUCTIVITY OF THE PLASMA MEDIUM

The charged particles that constitute the plasma will be under the effect of the Lorentz force when interacting with an electromagnetic wave. The effect of Lorentz force is given by:

$$\vec{F} = q\vec{E} + q(\vec{u} \times \vec{B})$$

2.1

where q is the charge of the particle, $\vec{u}$ is the velocity of the particle, $\vec{E}$ and $\vec{B}$ are the electric and magnetic fields influencing the particle.

For this initial analysis, it will be assumed that there is no static external electric and magnetic fields. If we take a transverse electromagnetic wave as in free space, the $\vec{E}$ and $\vec{B}$ fields are

$$\vec{E} = E_0 e^{j\omega t} \hat{a}_x \tag{2.2}$$

$$\vec{B} = \frac{E_0}{\dfrac{\eta_0}{\mu_0}} e^{j\omega t} \hat{a}_y \tag{2.3}$$

where μ_0 is the free space permeability constant and η_0 is the intrinsic wave impedance of free space. Note that, as we are interested only in the time dependence of the fields, e^{-jkz} term in the electric and magnetic field expressions is omitted as if it is included in the E_0 term.

The term $\dfrac{\eta_0}{\mu_0}$ can be rewritten as

$$\frac{\eta_0}{\mu_0} = \frac{\sqrt{\dfrac{\mu_0}{\varepsilon_0}}}{\mu_0} = \frac{1}{\sqrt{\varepsilon_0 \mu_0}} = c \tag{2.4}$$

where c is the speed of light in free space. Thus $\vec{B}$ can be expressed as

$$\vec{B} = \frac{E_0}{c} e^{j\omega t} \hat{a}_y \tag{2.5}$$

The resultant acceleration the particle undergoes is

$$\vec{a} = \frac{\vec{F}}{m} = \frac{q}{m} \left[\vec{E} + \left(\vec{u} \times \vec{B} \right) \right] \tag{2.6}$$

Writing the acceleration and velocity in differential form, and substituting equations 2.2 and 2.3 in equation 2.6, we get:

$$\frac{d^2 x}{dt^2} \hat{a}_x + \frac{d^2 y}{dt^2} \hat{a}_y + \frac{d^2 z}{dt^2} \hat{a}_z = \frac{q}{m} \left\{ E_0 e^{j\omega t} \hat{a}_x - \frac{E_0}{c} \frac{dz}{dt} e^{j\omega t} \hat{a}_x + \frac{E_0}{c} \frac{dx}{dt} e^{j\omega t} \hat{a}_z \right\} \tag{2.7}$$

Acceleration components can be written as:

$$\frac{d^2 x}{dt^2} = \frac{q}{m} E_0 \left(1 - \frac{1}{c} \frac{dz}{dt} \right) e^{j\omega t} \tag{2.8}$$

$$\frac{d^2 y}{dt^2} = 0 \tag{2.9}$$

$$\frac{d^2 z}{dt^2} = \frac{qE_0}{mc}\frac{dx}{dt}e^{j\omega t} \tag{2.10}$$

From the above equations we can obtain the velocity components for a charged particle. Assuming $\left|\dfrac{dz}{dt}\right| << c$, that is, velocity component of the particles along the direction of propagation is much smaller than the velocity of light, we have

$$\frac{d^2 x}{dt^2} = \frac{q}{m}E_0 e^{j\omega t}$$

Thus the velocity and displacement in the x-direction can be written as

$$\frac{dx}{dt} = \frac{qE_0}{m}\frac{1}{j\omega}e^{j\omega t} \tag{2.11}$$

$$x = -\frac{qE_0}{m\omega^2}e^{j\omega t} \tag{2.12}$$

In the formulations above, the integration constants are neglected, which are related to mean position and velocity of the charged particle during one period.

Substituting equation 2.11 in 2.10,

$$\frac{d^2 z}{dt^2} = \frac{qE_0}{mc}\frac{qE_0}{m}\frac{1}{j\omega}e^{j\omega t}e^{j\omega t} = \left(\frac{qE_0}{m}\right)^2\frac{1}{j\omega c}e^{j2\omega t} \tag{2.13}$$

$$\frac{dz}{dt} = \left(\frac{qE_0}{m}\right)^2\frac{1}{j\omega c}\frac{1}{2j\omega}e^{j2\omega t} = -\left(\frac{qE_0}{\omega m}\right)^2\frac{1}{2c}e^{j2\omega t} \tag{2.14}$$

$$z = -\left(\frac{qE_0}{\omega m}\right)^2\frac{1}{j4\omega c}e^{j2\omega t} \tag{2.15}$$

The above formulations show that the acceleration, velocity and position components of the particle are all periodic. This implies that the mean position, energy and velocity of particles are all constant for each period.

Having calculated the velocity components, it is now possible to express the volume current density induced within the plasma by the electromagnetic wave. The current density can be written as

$$\vec{J}_f = N_e q_e \frac{dx}{dt} \hat{a}_x$$

2.16

where N_e is the electron volume density of the plasma and q_e is the electron charge. In the above equation, it is assumed that the current flow is only in the x-direction, since the velocity of particles in the z-direction is negligible. Also the contribution of ion flow in the current density is neglected, for the ion mass is much greater than the electron mass. The particle mass term in the denominator of velocity expressions makes the velocity of ions much smaller than electron velocity, making the contribution of ions negligible. For example, for the argon molecule the ratio of ion mass to electron mass is

$$\frac{M_i}{m_e} = \frac{39,948 \times 1,6605 \times 10^{-27}}{9,109 \times 10^{-31}} = 7,2822 \times 10^4$$

where the particle masses have the unit of kg.

The volume current density can also be expressed directly in terms of electric field strength as

$$\vec{J}_f = \sigma \vec{E}$$

2.17

Equating the volume current density expressions in equations 2.16 and 2.17 and substituting the velocity expression from equation 2.11, we have

$$\sigma E_0 e^{j\omega t} \hat{a}_x = N_e q_e \frac{q_e E_0}{m_e} \frac{1}{j\omega} e^{j\omega t} \hat{a}_x$$

2.18

where m_e is the electron mass and N_e is the electron volume density of the plasma. From the equation above, the conductivity of plasma medium is found to be

$$\sigma = -\frac{j}{\omega} \frac{N_e q_e^2}{m_e}$$

2.19

The above expression is the conductivity expressed in terms of particle charge, mass and density. From the expression above it can be seen that conductivity

depends on the frequency of the electric field. As the frequency increases, the conductivity decreases due to the 1/ω term in the expression. This dependence of conductivity on the electromagnetic wave frequency is of great importance for the plasma antenna concept; physical parameters of the plasma will be determined according to the working frequency of the plasma antenna.

The imaginary conductivity means the current lags the electric field intensity by *π/2* radians, and the electron current is inductive. This means the scalar product ***E.J$_f$*** is also imaginary, and there is no energy loss in the medium. However we have assumed that there is no collision between electrons and other particles. Collision introduces a real part to the conductivity expression; medium absorbs energy in this case. More detailed analysis of the effects of collision is given in section 2.5.

2.3. PLASMA FREQUENCY

In order to understand the significance of equation 2.19, the natural behavior of the plasma medium must be inspected in detail. Being a medium of free charge carriers, plasma exhibits natural oscillations that occur due to thermal and electrical disturbances. Since we are mainly concerned with the motion of electrons within the plasma, we may focus on the harmonic oscillations of electrons around the ions for our analysis.

The derivation starts with the assumption that, due to the harmonic oscillation of electrons around ions, the electron density can oscillate at an angular frequency ω_p, and so the resulting electric field intensity $\vec{E}$ will oscillate at the same frequency [15]. The density oscillations give rise to a net free charge density ρ, which is related to volume current density $\vec{J}$ as

$$\nabla \cdot \vec{J} = -\frac{d\rho}{dt}$$

2.20

which is called the Continuity Equation. Taking $\vec{J}$ as in equation 2.17,

$$\nabla \cdot \left(\sigma\vec{E}\right) = \sigma\nabla \cdot \vec{E} = -\frac{d\rho}{dt}$$

2.21

The net free charge density ρ is related to the electric field intensity as

$$\nabla \cdot \vec{E} = \frac{\rho}{\varepsilon_0}$$

2.22

Thus, combining equations 2.19, 2.21 and 2.22, the free charge density ρ becomes

$$-\frac{j}{\omega} \frac{N_e q_e^2}{m_e} \frac{\rho}{\varepsilon_0} = -\frac{d\rho}{dt}$$

2.23

It must be noted that the contribution of ions to the plasma frequency is neglected. Being much heavier than electrons, the ion oscillation takes place in a much shorter span than electrons. Thus the volume charge density expression in equation 2.23 can be assumed to depend only on electron oscillation. The solution to the differential equation above is

$$\rho = \rho_0 e^{j\frac{N_e q_e^2}{\omega_p m_e \varepsilon_0}t}$$

2.24

The angular frequency of oscillation of the free charge density ρ is also ω_p, thus we have

$$\omega_p = \frac{N_e q_e^2}{\omega_p m_e \varepsilon_0} \Rightarrow \omega_p = \left(\frac{N_e q_e^2}{m_e \varepsilon_0}\right)^{\frac{1}{2}}$$

2.25

The plasma frequency can also be derived from the volume current density in the plasma due to electromagnetic wave interactions as

$$\vec{J}_t = \frac{\partial \vec{D}}{\partial t} + \vec{J}_f = j\omega\varepsilon_0\vec{E} - j\frac{N_e q_e^2}{\omega m_e}\vec{E}$$

$$= j\omega\varepsilon_0\vec{E}\left(1 - \frac{N_e q_e^2}{\omega^2 \varepsilon_0 m_e}\right) = j\omega\varepsilon_0\vec{E}\left(1 - \frac{\omega_p^2}{\omega^2}\right)$$

2.26

Thus the plasma frequency ω_p is found as in equation 2.25. Substituting the numerical values of parameters, we have the plasma frequency as

$$\omega_p = \left(\frac{N_e q_e^2}{\varepsilon_0 m_e}\right)^{1/2} = 8.94\sqrt{N_e}$$

2.27

where

9

$q_e = 1,60217653 \times 10^{-19} C$ is the electron charge,

$m_e = 9,1093826 \times 10^{-31} kg$ is the electron mass at rest,

$\varepsilon_0 = 8,8541878 \times 10^{-12} \dfrac{F}{m}$ Free space permittivity.

2.4. COMPLEX PERMITTIVITY OF THE PLASMA MEDIUM

Using the derived conductivity term in 2.19, the complex electric permittivity of the plasma medium can be calculated. The propagation constant of the electromagnetic wave in a conducting media can be obtained from the wave equations:

$$\nabla \times \nabla \times \vec{E} = -j\omega\mu_0\sigma\vec{E} + \omega^2\mu_0\varepsilon_0\vec{E} \qquad\qquad 2.28$$

$$\nabla \times \nabla \times \vec{H} = -j\omega\mu_0\sigma\vec{H} - \omega^2\mu_0\varepsilon_0\vec{H} \qquad\qquad 2.29$$

The solutions to the wave equations are

$$\vec{E} = E_0 e^{j(\omega t - kz)}\vec{a}_x \qquad\qquad 2.30$$

$$\vec{H} = \frac{E_0}{\eta} e^{j(\omega t - kz)}\vec{a}_y \qquad\qquad 2.31$$

where η is the intrinsic wave impedance of the medium and k is the propagation constant. Since we have started with the wave propagating in the z-direction, scalar propagation constant is used in our expressions instead of propagation vector. Substituting 2.30 in 2.28, the expression for the propagation constant is obtained as

$$k^2 = \omega^2\varepsilon_0\mu_0 - j\omega\sigma\mu_0 = \omega^2\varepsilon_0\mu_0\left(1 - \frac{j\sigma}{\omega\varepsilon_0}\right) \qquad\qquad 2.32$$

Since $k = \omega(\varepsilon\mu)^{\frac{1}{2}}$, the term in parentheses is the complex permittivity, which is

$$\varepsilon_r = \varepsilon_r' - j\varepsilon_r'' = \left(1 - \frac{j\sigma}{\varepsilon_0\omega}\right) = 1 - \frac{j}{\omega\varepsilon_0}\left(-j\frac{N_e q_e^2}{\omega m_e}\right) = 1 - \frac{\omega_p^2}{\omega^2} \qquad\qquad 2.33$$

and the propagation constant is

$$k = \omega \sqrt{\mu_0 \varepsilon_0 \left(1 - \frac{\omega_p^2}{\omega^2}\right)}$$ 2.34

As seen above, the propagation constant depends on the relation between the plasma frequency and wave frequency.

2.5. EFFECTS OF ELECTRON-NEUTRAL COLLISION

During the derivations of previous sections, it was assumed that there is no loss of energy of electrons due to collisions between electrons and other particles constituting the plasma. However, with increasing plasma pressure and electron number density the rate of such collisions increase such that they are no more negligible. Of these collision mechanisms, the greatest amount of energy is lost due to the electrons colliding into electrically neutral particles within the plasma; from here after this collision event is referred as "electron-neutral collision".

The electron-neutral collision, being a mechanism of energy loss, can be inserted into the previous equations by building an equation of forces acting on the electrons. The initial equation, disregarding the collisions, is

$$m_e \frac{d^2 x}{dt^2} = -q_e E_0 e^{j\omega t}$$ 2.35

where m_e is the electron mass, q_e is the electron charge and $E_0 e^{j\omega t}$ is the time-harmonic electric field acting on the electron. Expressing $\frac{d^2 x}{dt^2}$ in terms of electron velocity,

$$\frac{d^2 x}{dt^2} = \frac{d}{dt}\frac{dx}{dt} = \frac{d}{dt}V$$

and writing equation 2.35 in phasor notation, neglecting the components of the electron velocity transverse to electric field direction, we get

$$j\omega m_e V_e = -q_e E_0$$ 2.36

11

The electron-neutral collision can be inserted into this force equation as an average damping force so that

$$j\omega m_e V_e = -q_e E_0 - F_d \qquad 2.37$$

where F_d is the damping force resulting from the electron-neutral collision. The damping force can be expressed in terms of electron momentum as

$$\vec{F}_d = \int_{t'=0}^{t} m_e \vec{V}_e(t')dt' \qquad 2.38$$

We may assume that the momentum of the electrons after collision is zero. Thus the integral in the equation above can be solved for unit time (1 second) to yield

$$\vec{F}_d = \nu m_e \vec{V}_e(0) \qquad 2.39$$

where ν is the collision frequency and $\vec{V}_e(0)$ is the average electron velocity before the collision. Combining equations 2.37 and 2.39, we get

$$j\omega m_e V_e = -q_e E_0 - \nu m_e V_e \qquad 2.40$$

The collision frequency can be expressed as

$$\nu = N.\sigma_c(V).V \qquad 2.41$$

where N is the volume density of the background medium and $\sigma_c(V)$ the cross section of the particle with velocity V for the type of collision being considered. The particle cross sections depend on the energy and type of the particles, the exact relationship is out of the scope of this thesis.

The electron velocity can be extracted from equation 2.40 as

$$V_e = \frac{-q_e E_0}{(j\omega + \nu)m_e} \qquad 2.42$$

which is then submitted into equation 2.16 to obtain

$$\vec{J}_f = \frac{-Nq^2 E_0}{m(j\omega + v)}\hat{a}_x$$ 2.43

From the equation above, the conductivity term modified by the electron-neutral collision is given as

$$\sigma = -\frac{j}{(\omega - jv)}\frac{Nq^2}{m}$$ 2.44

and the complex permittivity of plasma medium is modified as

$$\varepsilon_r = \varepsilon_r' - j\varepsilon_r'' = \left(1 - \frac{j\sigma}{\varepsilon_0\omega}\right) = 1 - \frac{j}{\omega\varepsilon_0}\left(-j\frac{Nq^2}{(\omega - jv)m}\right) = 1 - \frac{\omega_p^2}{\omega(\omega - jv)}$$ 2.45

2.6. FREQUENCY DEPENDENT NATURE OF INTERACTION

We have derived the complex permittivity and conductivity in terms of plasma frequency, collision frequency and wave frequency. In this section, interaction of electromagnetic waves and plasma medium will be inspected by examining the propagation constant, intrinsic wave impedance and conductivity.

In equation 2.45, the propagation constant for negligible electron-neutral collision is given as

$$k = \omega\sqrt{\mu_0\varepsilon_0\left(1 - \frac{\omega_p^2}{\omega(\omega - jv)}\right)}$$

where ω_p is the plasma frequency and ω is the electromagnetic wave frequency. Thus the solution of wave equation is

$$\vec{E} = E_0 e^{j\omega t} e^{-j\omega\sqrt{\mu_0\varepsilon_0 k}}\vec{a}_x$$ 2.46

Neglecting the collision frequency, it can clearly be seen that for $\omega < \omega_p$ the propagation constant is imaginary. The exponential term with real exponents means the electromagnetic wave is evanescent in the plasma medium. Thus there are two cases for propagation of electromagnetic waves in plasma medium.

$\omega > \omega_p$: The propagation constant is real, and the wave propagates in the plasma. In such cases, the plasma medium has dielectric properties, which are controllable electrically.

$\omega < \omega_p$: The propagation constant is imaginary; the wave is evanescent within the plasma medium. The wave may either be reflected or absorbed in this case, depending on the electron collision frequency.

The conductivity term, as given in equation 2.44, shows that the conductivity depends very much on electron collision frequency. A high collision frequency lowers the real part of the conductivity, at the same time increasing the imaginary part of the propagation constant. Thus, the plasma with high collision frequency behaves as a lossy medium.

2.7. EFFECTS OF MAGNETIC FIELD ON PLASMA-WAVE INTERACTION

Plasma, which is made up of charged particles, interacts strongly with magnetic fields. Magnetic fields are used to direct the plasma flow or confine the hot plasma in fusion research. In antenna applications, it may be desirable to confine the plasma so as to obtain various plasma medium geometry specific to the intended application. Thus the effect of permanent magnetic fields on plasma-electromagnetic wave interaction is important in antenna applications.

The interaction of electromagnetic waves with magnetized plasmas can be inspected according to the wave polarization. Neglecting electron-neutral collision, the refractive index of the magnetized plasma is given by the Appleton-Hartree formula [19]:

$$n_{\frac{1}{2}}^2 = 1 - \frac{\omega_p^2}{\omega^2 - \dfrac{\omega^2 \omega_t^2}{2(\omega^2 - \omega_p^2)} \pm \sqrt{\left[\dfrac{\omega^2 \omega_t^2}{2(\omega^2 - \omega_p^2)}\right]^2 + \omega^2 \omega_l^2}} \qquad 2.47$$

where ω_t is the transverse gyrofrequency, ω_l is the longitudinal gyrofrequency, and ω_p is the plasma frequency. The reference for the terms "transverse" and "longitudinal" is the direction of propagation of the electromagnetic wave in plasma

medium. The subscripts 1 and 2 of the refractive index symbol are for ordinary and extraordinary rays respectively. Appleton-Hartree formula implies that the magnetized plasma is an anisotropic medium, and the relative permittivity is a tensor in this case.

In our case we are interested in waves traveling in a transverse magnetic field. Thus we may take $\omega_l = 0$ in equation 2.47. Then the equation becomes

$$n_1^2 = 1 - \frac{\omega_p^2}{\omega^2} \qquad\qquad 2.48$$

$$n_2^2 = 1 - \frac{\omega_p^2}{\omega^2 - \dfrac{\omega^2 \omega_t^2}{\omega^2 - \omega_p^2}} \qquad\qquad 2.49$$

The equation 2.48 is for the ordinary wave, which has an electric field parallel to the permanent magnetic field. Thus the ordinary wave is not affected by the permanent magnetic field. However, the extraordinary wave, which has an electric field perpendicular to the permanent magnetic field, is strongly affected by the magnetic field, as seen in equation 2.49.

The cause of the magnetic field's strong effect on the transverse electric field is that the magnetic field prevents electron motion in the perpendicular direction. Thus, the electron mobility perpendicular to the magnetic field decreases, resulting in a change in the relative permittivity and refractive index for the extraordinary wave. The refractive index for the extraordinary wave decreases with increasing magnetic field intensity.

2.7.1. CONFINEMENT OF PLASMA IN MAGNETIC FIELD

The plasma can be shaped into specific geometries to match the needs of the intended application by magnetic confinement. Confinement is a state where the particles in the plasma are bounded to a region in space, and the criterion for the confinement depends on the application.

The confinement is achieved by the cyclic motion of charged particles due to the magnetic field. Thus the magnetic field prevents the particle motion in the transverse

direction. The gyroradius and gyrofrequency of particles are the criterion of confinement usually. The gyrofrequency is depends on the magnetic field strength, however, the gyroradius depends on both the magnetic field strength and electron temperature.

The gyrofrequency and gyroradius can be calculated for a uniform magnetic field $\vec{B}$ and electron velocity $\vec{v}$ in the transverse direction. The force exerted on the electron, with electric charge q, by the magnetic field is:

$$\vec{F} = q\vec{v} \times \vec{B}$$
2.50

The centrifugal force on a particle in circular motion is:

$$F = m\frac{v^2}{r}$$
2.51

where m is the particle mass and r is the gyroradius.

The magnitude of magnetic force can be taken equal to the centrifugal force, assuming the electrons are in circular motion. Also since we have assumed the velocity vector and magnetic field vector are vertical

$$\vec{v} \times \vec{B} = \left|\vec{v}\right|\left|\vec{B}\right| = vB$$
2.52

Thus equating 2.50 to 2.51, we get

$$qvB = m\frac{v^2}{r}$$
2.53

From equation 2.53, we may obtain the gyroradius expression:

$$r = m\frac{v}{qB}$$
2.54

The electron velocity can be calculated from electron energy, which can be measured by Langmuir Probe. The electron energy is determined in terms of electron-volts (eV). 1 eV is the energy gained by a single unbound electron when it falls through an electrostatic potential difference of one volt.

16

The electron velocity can be expressed in terms of the total path the electron travels in one period:

$$v = \frac{2\pi r}{\tau}$$

2.55

Substituting equation 2.54 in equation 2.55:

$$v = \frac{2\pi m v}{qB\tau}$$

2.56

Then the gyrofrequency of the electron is

$$f = \frac{1}{\tau} = \frac{qB}{2\pi m}$$

2.57

CHAPTER 3

GENERATION OF PLASMA BY DC DISCHARGE

3.1.   INTRODUCTION

The first studies on the plasma medium are conducted on the DC discharge systems. A DC discharge system is basically applying a constant electric field on a low-pressure gas via electrodes of various physical properties. While explanation of the DC discharge setup is so simple, the mechanism underlying the discharge and explanation of behavior of the plasma medium in the discharge is quite complex.

Our inspection will be limited to those properties that helps us calculate the electrical circuitry parameters required to form a plasma medium with the properties desired for the interaction with the electromagnetic waves. The electrical circuitry parameters we are interested in are the voltage-current characteristics and the current required to reach a desired electron number density.

3.2.   QUALITATIVE INSPECTION OF DC DISCHARGE

The regions in the DC discharge are formed because of the mobility difference between the electrons and ions; electrons move much faster than ions under the effect of applied electric field. Due to this mobility difference, the contribution of ions to current densities and conductivity was neglected in the interaction of plasma with electromagnetic waves. The same mobility difference gives rise to the regions called *sheath regions*.

After the gas is ionized, the electrons in the cathode region are repelled by the negative charge of the cathode, while ions are attracted to the cathode. Since the ions are much heavier than the electrons, the electrons will move away from the cathode very rapidly while ions take a longer time to reach the cathode. Due to this difference in the mobility of electrons and ions, a region with a net positive charge forms in front of the cathode.

Similarly the anode repels the ions with its positive charge while attracting the electrons. Due to the same mobility difference, the electrons are consumed by the anode much faster than the ions can move away from the vicinity of the anode. This effect forms another region with a net positive charge in front of the anode. The two regions in front of the electrodes with a net positive charge are called the sheath regions.

Sheath regions are formed even in the situation of existence of conductive walls within an ionized gas, for the electrons will collide more frequently with the wall than ions. This process will charge the conductive wall negatively, repelling all other electrons in the vicinity and leaving a positively charged gas blanket in front of the wall. Effectively the plasma will appear as if it has a positive potential with respect to surrounding areas.

Between the sheath regions, there is an ionized region where the overall charge is neutral. This region, having a positive potential as explained above, is called *the positive column*. In positive column the electric field intensity is very low. The *E.J* energy is consumed by collision of particles with each other and with the surrounding chamber walls. As the positive column can extend almost without limit, it is the region of the DC discharge that is to be utilized as a radiator or a reflector in plasma antenna applications.

3.3. SHEATH REGION

Experiments with the DC discharges show that most of the voltage drop across a DC discharge occurs in the cathode sheath. Also since the ion flux dominates the current in the sheath region; it is much easier to calculate the current passing through the DC glow by calculating the ion flow in the sheath region. The voltage and current calculations in the sheath region may give an approximate value for voltage and current required to drive a DC discharge with the required electron density in the positive column region.

Thus characteristics of the DC discharge may be analyzed easily by inspecting the sheath regions. When only a fraction of molecules in a gas is ionized, the resulting plasma is described as "cold plasma". In cold plasma, the particle collisions can be neglected. The plasma that we are interested in is "cold" and ions move much slower

than the electrons. To simplify the calculations and formulations is assumed that there is negligible collision between particles. Also in the cathode sheath region, there is negligible ionization, recombination and collision of particles.

The aim of calculations is to find a relationship between the electron number density n_e and the current density $\vec{J}$ passing through the plasma medium by making use of the rule that charge of the sheath region is always positive. The reason for the sheath region's being positively charged is given in section 3.2.

The ion flux in the sheath region is constant due to the conservation of charge. This can be formulated as

$$n_i(x)u(x) = n_{is}u_s \qquad\qquad 3.1$$

where $u(x)$ is the ion velocity within the sheath, u_s is the ion velocity at the sheath edge, n_{is} is the ion density at the sheath edge and $n_i(x)$ is the ion density within the sheath. The condition of negligible collision means the ion energies are conserved. Ion energy depends on the initial energy at the sheath edge and the potential difference between the sheath edge and ion position within the sheath. In cold plasma ions are not relativistic, so the kinetic energy of the ion can be written as

$$\tfrac{1}{2}Mu^2(x) = \tfrac{1}{2}Mu_s^2 - q\Phi(x) \qquad\qquad 3.2$$

where $\Phi(x)$ is the potential difference with respect to sheath edge. From equation 3.2, the ion velocity $u(x)$ is

$$u^2(x) = u_s^2 - \frac{2q\Phi(x)}{M} \qquad\qquad 3.3$$

Submitting equation 3.3 in to equation 3.1 and solving for $n_i(x)$, the ion density is expressed as

$$n_i = n_{is}\left(1 - \frac{2q\Phi}{Mu_s^2}\right)^{-\tfrac{1}{2}} \qquad\qquad 3.4$$

The electron density is obtained by assuming that the electrons move into the sheath region by diffusion. The concentration at any location is proportional to the

20

electron energy at that location divided by the electron thermal energy. Thus the electron density is given by [14]

$$N_e(x) = n_{es} e^{q\Phi(x)/kT_e}$$

3.5

The electron and ion densities are equal to each other in the positive column region of the plasma, which is assumed to start at the sheath edge. Thus at the sheath edge $n_{es} \equiv n_{is} \equiv n_s$. However, within the sheath region the ion density must always be greater than the electron density at every location. Both ion and electron densities decrease as we get closer to cathode, thus the condition can be formulated in terms of rate of change of particle densities as

$$\frac{d}{dx} n_i < \frac{d}{dx} N_e$$

3.6

Replacing n_i and N_e by 3.4 and 3.5 respectively, the condition becomes

$$\frac{d}{dx}\left\{ n_{is}\left(1 - \frac{2q\Phi}{Mu_s^2}\right)^{-1/2}\right\} < \frac{d}{dx}\left\{ n_{es} e^{q\Phi(x)/kT_e}\right\}$$

$$\left(1 - \frac{2q\Phi}{Mu_s^2}\right)^{-3/2} \frac{qn_{is}}{Mu_s^2}\frac{d}{dx}\Phi < \frac{n_{es} e^{q\Phi(x)/kT_e}}{kT_e}\frac{d}{dx}\Phi$$

3.7

$\Phi = \Phi(x)$ is defined as the potential difference with respect to sheath edge, thus at the sheath edge the $\Phi(x)$ terms become zero. The electron and ion charge term q, the ion and electron densities and the derivatives of $\Phi(x)$ cancel out, thus equation 3.7 becomes

$$\frac{1}{Mu_s^2} < \frac{1}{kT_e}$$

3.8

The ion velocity term can be extracted from this inequality as

$$u_s > \sqrt{\frac{kT_e}{M}} = u_B$$

3.9

where $k = 1{,}381 \times 10^{-23} \, J / K$ the Boltzmann constant, T_e is the electron temperature in Kelvin, u_b is the Bohm velocity, and the inequality is called *Bohm Sheath Criterion*. The term kT_e represents the electron energy, which can be measured experimentally in terms of eV, standing for *"electron volts"*. One eV is the amount of energy gained by a single unbound electron when it falls through an electrostatic potential difference of one volt. In order to obtain the Bohm velocity in units of m/s, the energy must be represented in terms of Joule. The relationship between eV and Joule is

$$1eV = 1{,}60217653 \times 10^{-19} \, J \qquad\qquad 3.10$$

The Bohm Sheath Criterion indicates that the ions must have a certain velocity at the sheath edge, thus there must be a region in which there is a finite electric field that accelerates the ions to the required velocity. This region is called *presheat* region, which is typically much wider than the sheath.

From the electron density expression, it can be assumed that the electron density on the cathode is negligible, such that the current flowing through the plasma can be calculated from the Bohm velocity of ions at the sheath edge. The ion flux at the sheath edge must be equal to the ion flux on the cathode surface, as expressed before, and thus the current density is

$$J_0 = q n_s u_B = q n_s \left(\frac{kT_e}{M} \right)^{1/2} \qquad\qquad 3.11$$

The current density expression in equation 3.11 is indeed the current density in the sheath edge. The current in the sheath edge is almost purely due to the ion flow. The reason the above formula holds is that the plasma column radius is assumed to be constant along the discharge; and the system is assumed to be in a steady state, where there is no change in charge density along the plasma column. In such a case, due to the conservation of charge, the current density along the discharge may not change.

3.3.1. CALCULATION OF CURRENT REQUIREMENT

The current density in the plasma medium is expressed in terms of ion density in the sheath edge, ion mass and electron energy in equation 3.11. The aim is, however, to obtain a relationship between the plasma frequency and the current density. The electron density can be expressed in terms of plasma angular frequency by modifying equation 2.27

$$\omega_{pe}^2 = \left(2\pi f\right)^2 = \frac{N_e q_e^2}{m_e \varepsilon_0} \Rightarrow N_e = \frac{\omega_{pe}^2 m_e \varepsilon_0}{q_e^2} \qquad\qquad 3.12$$

In equation 3.11, the ion density at the sheath edge is equal to the electron density in the positive column. Thus the ion density term in equation 3.11 can be replaced by the electron density term in equation 3.12 to obtain

$$J_0 = q n_s u_B = \frac{\omega_{pe}^2 m_e \varepsilon_0}{q}\left(\frac{kT_e}{M}\right)^{\!\!1/2} \qquad\qquad 3.13$$

Our plasma is generated from the Argon gas, thus the ion mass term in the formulation is the atomic mass of Argon. Thus, the required parameters for calculations are:

$1eV = 1,60217653 \times 10^{-19}$ Joule

$q = 1,60217653 \times 10^{-19}$ Coulomb

$M_{Ar} = 39,948 AMU = 6,633520637928 \times 10^{-26}$ kg

$m_e = 9,1093826 \times 10^{-31}$ kg

$\varepsilon_0 = 8,8541878 \times 10^{-12}$ Farad/meter

From equation 3.12, the critical electron density of plasma for a given frequency is

$$N_e = \frac{(2\pi)^2 \times 9{,}1093826 \times 10^{-31} \times 8{,}8541878 \times 10^{-12}}{(1{,}60217653 \times 10^{-19})^2} f^2 = 0{,}0124044 f^2 = \frac{f^2}{80{,}616386}$$

3.14

where the unit for density is $1/m^3$.

The required current density for a given plasma frequency and for electron energy of 1 eV can be calculated from equation 3.13 as

$$J_0 = \frac{f^2}{80{,}616386} \times 1{,}60217653 \times 10^{-19} \left(\frac{1{,}60217653 \times 10^{-19}}{6{,}633520 \times 10^{-26}} \right)^{\frac{1}{2}} = 3{,}08837 \times 10^{-18} f^2$$

3.15

where the unit for current density is A/m^2. For a plasma frequency of 1 GHz, the required current density is

$$J_0 = 3{,}08837 \times 10^{-18} \times (10^9)^2 = 3{,}088 A/m^2$$

and for a tube of cross sectional area 10cm^2, the required current is

$$I = J_0 \times A = 3{,}088 \times 10^{-3} \cong 3mA$$

For the plasma medium to be used in microwave frequencies, the plasma density must be much higher. For example, the required current density for a plasma frequency of 10 GHz is

$$J_0 = 3{,}08837 \times 10^{-18} \times (10^{10})^2 = 308{,}8 A/m^2$$

and for a tube of cross sectional area 10cm^2, the required current is

$$I = J_0 \times A = 308{,}8 \times 10^{-3} \cong 308mA$$

The relationship between the current density and the plasma frequency is given in Figure 3.1.

Figure 3.1: Plasma frequency vs current density, the current density increases with the square of plasma frequency

3.3.2. THE VOLTAGE REQUIREMENT

The voltage requirement of DC discharge plasma depends on the gas and electrode material utilized in plasma generation, discharge length, and the current density. The experimental data shows that the two important criteria are the voltage required for ignition of plasma and the voltage required to obtain the required current density.

From experimental data it is found that the ignition voltage required for Argon at 1 Torr pressure is around 1000V, while the ignition voltage for air at 1 Torr is around 2000V for the discharge setup used in our experiments. The current density required for our experiments could be achieved at a discharge voltage of 2000V for Argon at 1 Torr, and 3000V for air at 1 Torr.

CHAPTER 4

EXPERIMENTS ON THE INTERACTION OF PLASMA AND ELECTROMAGNETIC WAVES

4.1. INTRODUCTION

Theoretical study of the interaction of plasma medium with electromagnetic waves has been introduced in the previous sections. The possibility of plasma antenna concept has been verified in this manner. However, to be of use in practical applications, feasibility of plasma systems must be demonstrated. Such a demonstration requires experimentation on basic wave-plasma interaction.

The experimental setup basically consists of a plasma generating apparatus, antennas of appropriate frequency range and microwave measurement devices. The plasma in our experimental setup is subjected to microwaves, and various measurements are conducted to show the interaction between plasma medium and electromagnetic waves is realizable.

4.2. PLASMA GENERATING APPARATUS

The plasma generating apparatus can take many shapes and can include various components, depending on the parameters of plasma that are specific to application. In our experimental setup, DC discharge plasma at 1 Torr (1 mm Hg) pressure is generated as the interacting medium. Such plasma is much simpler to generate compared to other methods, the required voltages to ignite and sustain the discharge are quite low compared to other pressure ranges [2-7, 13].

The plasma generation apparatus consists of an air-tight tube, a vacuum pump, a vacuum gauge to measure the pressure, two electrodes on each end of the tube, and DC discharge circuitry. The complete apparatus can be seen in Figure 4.1. The vacuum pump must be able to reach pressures on the order of mTorr scale, especially if the gas used in the plasma generation is different from air.

Figure 4.1: The plasma generating apparatus.

4.2.1. SELECTION OF ELECTRODES AND GASES

Brass electrodes and air is used in the experimental setup initially. The brass cathode, due to continuous ion bombardment, suffered from a phenomenon called sputtering. Sputtering is the coating of inner walls of the plasma chamber with the cathode material. Although sputtering is a technique widely used in material processing, metallic coating of the plasma tube is an undesired feature in plasma antenna applications. The metallic coating not only degrades the DC discharge by initiating break-downs at very low voltage levels, but also interferes with the microwave in an undesired manner.

Sputtering requires ion energies above a threshold and the heating of the cathode by the continuing ion bombardment. Brass, being a very soft metal, quickly erodes under the ion bombardment. The resulting metallic coating can only be wiped off the chamber walls by strong acids such as HCl with 15% volume density. Instead of brass, steel or aluminum can be used. Staining of steel degrades the discharge by deteriorating the discharge homogeneity. Thus, aluminum was used in the experimental setup as electrode.

Different gases have different voltage requirements to reach a specific current value. Each gas has a different ignition voltage depending on the gas pressure, and mixtures of gases may have completely different discharge characteristics. For the sake of commercial availability and low voltage requirement, Argon plasma is preferred. Air at 1 Torr pressure requires a voltage about 3000V to generate a current density of 250A/m^2 through the plasma, while only 2000V was enough with Argon.

4.2.2. DC DISCHARGE CIRCUITRY

Due to the high voltage and current levels required for the generation of plasma, DC generators with the required voltage and current capability were not commercially available. Thus a DC supply had to be built from a transformer, a bridge diode and capacitor banks. The voltage-current characteristics of the plasma discharge required adjustable resistor banks as well. The combined DC discharge circuitry is given in Figure 4.2. Current passing through the discharge is adjusted by Variac in the transformer input and resistor block connected in series to the discharge tube.
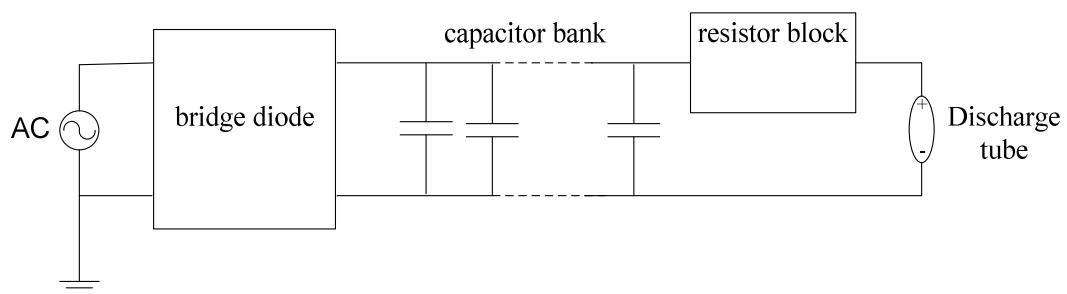
Figure 4.2: The discharge circuit. Bridge diodes and capacitor banks form the DC power supply. The circuit is fed by a high voltage transformer, which is adjusted by a Variac

4.2.2.1. VOLTAGE-CURRENT CHARACTERISTICS OF DISCHARGE PLASMA

The DC discharge plasma mainly has 4 stages, each of which having different voltage-current characteristics.

1. Ignition: The gas, when not ionized, acts as an insulator between the electrodes. As the electric field intensity increases the electrons are ripped off

the atoms, resulting in the ionization of the gas and a sudden increase in the conductivity of the gas. Without limiting resistors connected in series to the discharge tube, the current level increases very rapidly, resulting in either damage in the circuitry, or ceasing of the operation due to drained capacitor banks.

2. Normal Glow: After the ignition, if the current levels are controlled appropriately, the discharge may enter the normal glow stage. At this stage, the current level changes very much even with the slight changes in discharge voltage. This state is not suitable for plasma antenna operation, for the electron density of the plasma is prone to change very much with small fluctuations in the discharge voltage.

3. Abnormal Glow: After a certain current level, slope of the voltage-current characteristic curve increases. Voltage must be increased considerably to increase the current passing through the plasma. This stage is the most suitable for our continuous DC discharge plasma, for the electron density in the plasma is not affected very much from the fluctuations in the discharge voltage.

4. Break-Down: Conductivity of the plasma increases very suddenly and irreversibly after some electric field intensity specific to the setup. Once a discharge enters breakdown, the only way to establish normal operation is to extinguish and reignite the plasma. This mode of operation must be avoided, for the sudden and uncontrolled increase in current levels may damage the discharge circuitry. Current limiting resistor bank is a method of preventing breakdowns, and may provide circuit protection in case of breakdowns by discharging the capacitors in a controlled manner.

4.2.2.2. DISCHARGE CURRENT CONTROL

As expressed above, the aim of the resistor block is to prevent the discharge from entering the breakdown stage by limiting the current. However the current limiting requirements for the ignition phase and the experimentation phase are different, thus, the current limiting resistor bank has to be adjustable. For this purpose, the resistor configuration given in Figure 4.3 is designed and implemented. The resistor block

consisted of 16 resistors with 6,8kΩ resistance and 50W rated power. The resistors are connected in parallel configuration in groups of 4, thus effectively there are 4 resistors with 1,7kΩ resistance and 200W rated power.
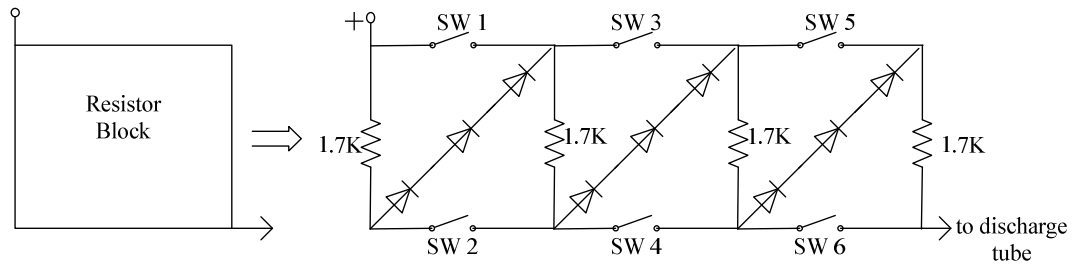

Figure 4.3: The current limiting resistor block. The resistor configuration can be changed by switches (SW1-SW6).

In the ignition phase, the resistor block must be able to withstand the full voltage that is applied to the tube, in case there is a breakdown. The voltage required for the ignition is around 2000V for air and around 1000V for Argon at a pressure of 1 Torr. Since the initial setup used air, resistor block was built so as to withstand a higher voltage level. The first stage had a maximum current capacity of 340mA with 2312V voltage drop on the resistors. With an ignition voltage of 2000V, this resistor block is able to prohibit the high currents of a break-down mode. This mode of operation is achieved with all switches open.

During the experimental operation, a higher voltage level is needed on the tube. The resistor block, therefore, must be able to withstand the required current level without too much voltage drop on it. The resistance value must be decreased by adjusting the resistor block. The highest current the designed resistor block could withstand was calculated to be 680mA with a voltage drop of 1156V on the resistors. This current is already more than that could be supplied to the discharge tube without initiating a break-down while using Argon. This mode of operation is achieved with SW1, SW2, SW4, and SW6 closed.

A third stage, with minimum voltage drop and very high current capacity, could be implemented with minimal effort due to resistor block design. Thus to have the ability to test the system at a broader range of voltages and currents, the third stage

30

with a maximum current of 1360mA with a voltage drop of 587V is implemented. This mode of operation is achieved with all switches closed.

4.2.2.3. CAPACITOR BANKS

The current requirement of the DC discharge is calculated in section 3.3.1. Considering the previous experiments [2-7], the voltage requirement of the system for maximum current level was deduced to be around 2000V. Using the commercially available 100μF-400V capacitors, a capacitor bank with 3200V maximum voltage capability is assembled.

Figure 4.4: Capacitor bank of the DC power supply has a capacitance of 150μF, maximum voltage of around 3000VDC.

4.2.3. STRIATION EFFECT

To be able to conduct microwave reflection experiments, plasma with sheet geometry is more suitable compared to plasma with cylindrical geometry. Magnetic fields and rod shaped electrodes are used to obtain plasma sheet in [2-7]. To obtain a simpler geometry and due to the available setup size, two glass plates are inserted into cylindrical chamber on each side of rod shaped electrodes. The glass plates prevented the plasma from diffusing into the cylindrical chamber, limiting the plasma in a sheet shaped geometry of 1cm thickness.

The decreased chamber cross section resulted in a phenomenon called striation effect, which is given in Figure 4.5. The voltage required to obtain the desired

current density increased significantly due to the increased rate of particle collision with the chamber walls. Therefore plasma electron densities required for microwave reflection could not be reached.
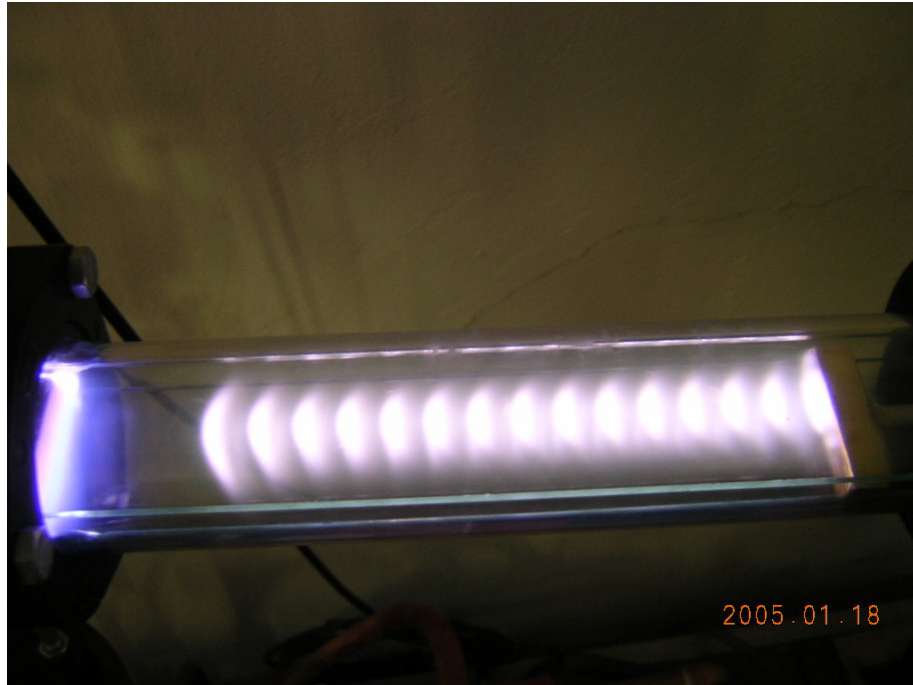
Figure 4.5: The initial plasma tube with glass plates, striations in the plasma are visible in this figure.

The striation phenomenon limits the pressure range that can be used for a specific chamber size. Striations can be observed in long chambers with narrow cross sections and low plasma pressures. Thus, chamber dimensions must be chosen accordingly.

4.3. MICROWAVE EXPERIMENTS ON DC DISCHARGE PLASMA

The most significant parameter that governs the interaction of plasma medium and electromagnetic waves is the plasma frequency. As given in section 2.6, the relation between the plasma frequency and wave frequency determines the behavior of plasma medium. The aim of microwave experiments on the plasma medium is to demonstrate the effect of plasma frequency.

For this aim, two experiments have been conducted. The first experiment was aimed to show that plasma becomes opaque for the microwave frequencies below the

plasma frequency, while the objective of second experiment was to demonstrate the microwave reflection from a plasma column. In literature it has been found out experimentally that while microwave cut-off can be obtained by plasma with frequency equal to that of microwave, reflection quality equivalent to a metallic sheet required a plasma frequency of at least $\sqrt{2}$ times higher than wave frequency.

4.3.1. MICROWAVE CUT-OFF EXPERIMENTS

The setup for microwave cut-off experiments consisted of two horn antennas of appropriate frequency range facing each other, with the cylindrical discharge tube in between them. Transmission loss S_{21} between the two horns is measured using a sweep signal generator and a network analyzer. The cut-off experiment configuration is given in Figure 4.6 and Figure 4.7.
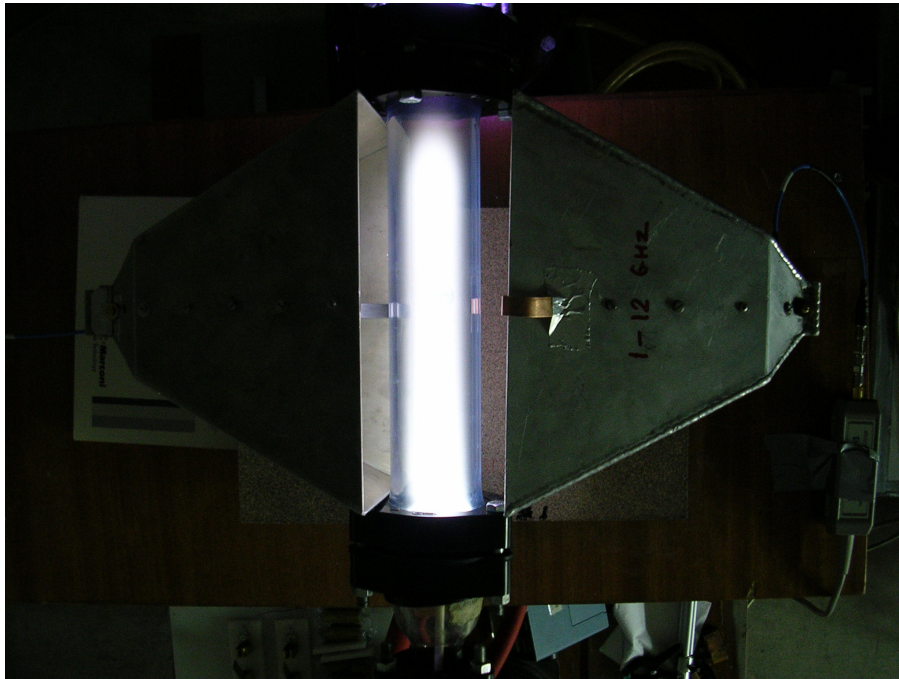
Figure 4.6: Microwave cut-off experiment setup

PLASMA TUBE

DETECTOR
HP 85025D

5757C

SWEEPER
83640A

PLOTTER
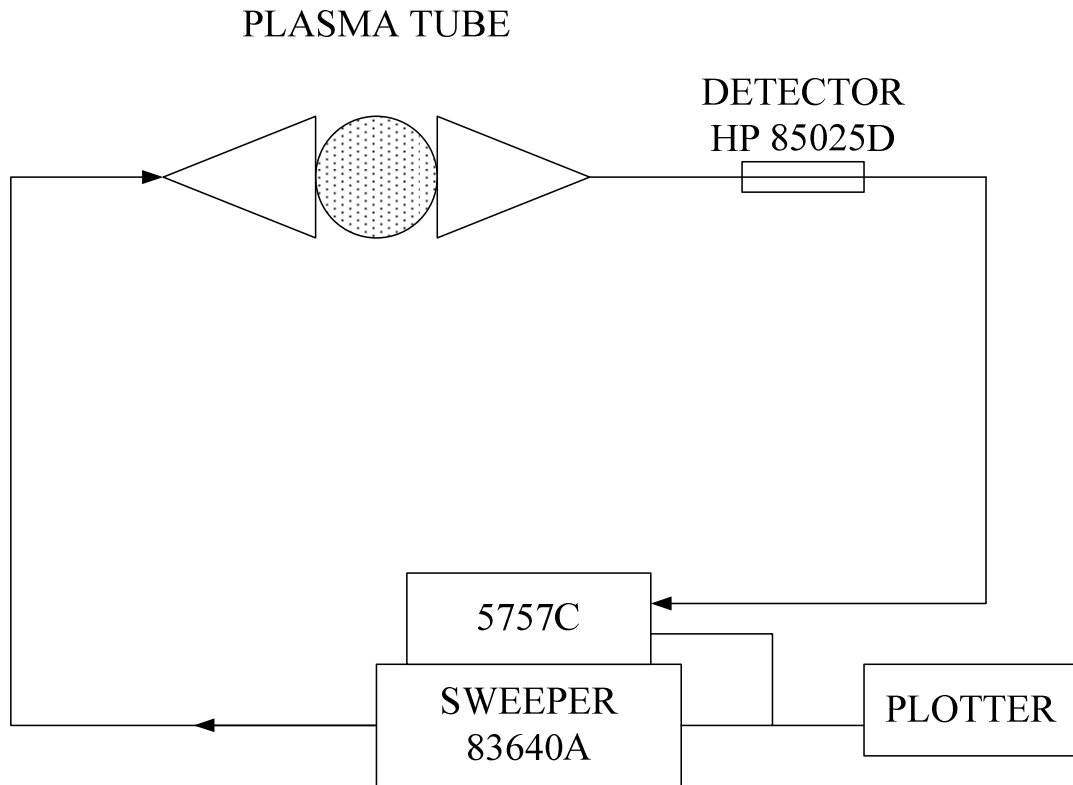
Figure 4.7: Microwave cut-off experiment setup

The calculated plasma frequency for a current density of $250A/m^2$ is about 9 GHz. The results of the experiments show very significant transmission loss at low frequencies, especially up to 4 GHz. Attenuation can be observed up to 8 GHz with less transmission loss for higher frequencies due to non-uniform plasma electron density. The plasma electron density has a radial gradient, with electron density decreasing towards the chamber walls. The decreasing plasma electron density in the radial direction results in smaller plasma region with enough electron density to cut-off the higher frequencies. The results are given in Figure 4.8, Figure 4.9, Figure 4.10, and Figure 4.11.
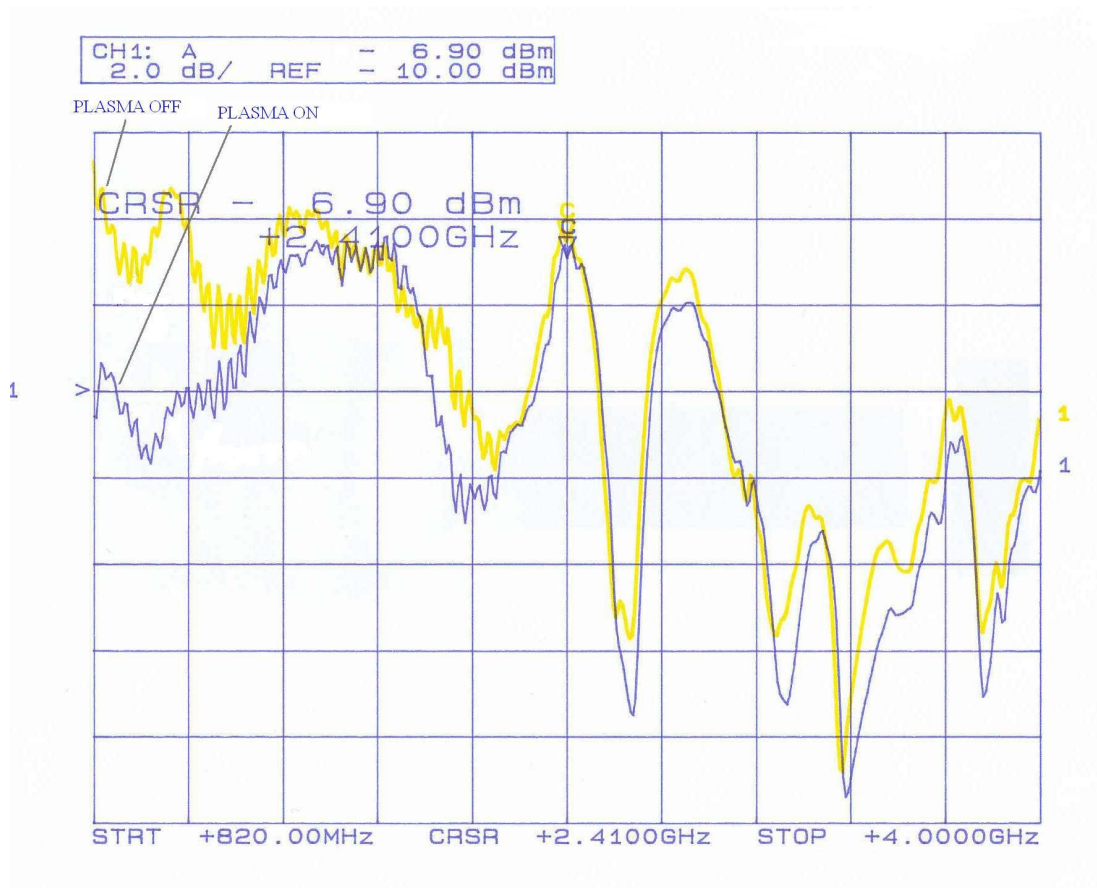
Figure 4.8: Effect of plasma on transmission loss for the frequency range of 820MHz-4GHz, with scale 2dB/div, for antenna polarization vertical to tube orientation.

CRSR —   7.10 dBm
        +2.4100GHz

PLASMA OFF

PLASMA ON

1

STRT   +820.00MHz   CRSR   +2.4100GHz   STOP   +4.0000GHz

1
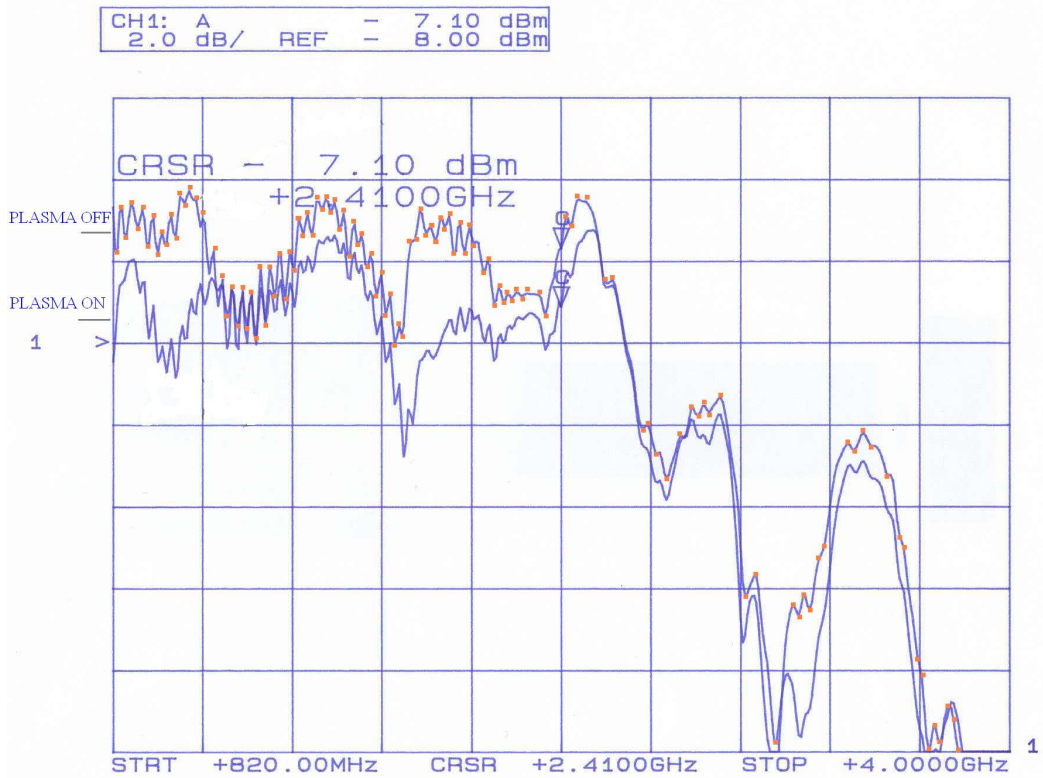
Figure 4.9: Effect of plasma on transmission loss for the frequency range of 820MHz-4GHz, with scale 2dB/div, for antenna polarization parallel to tube orientation.
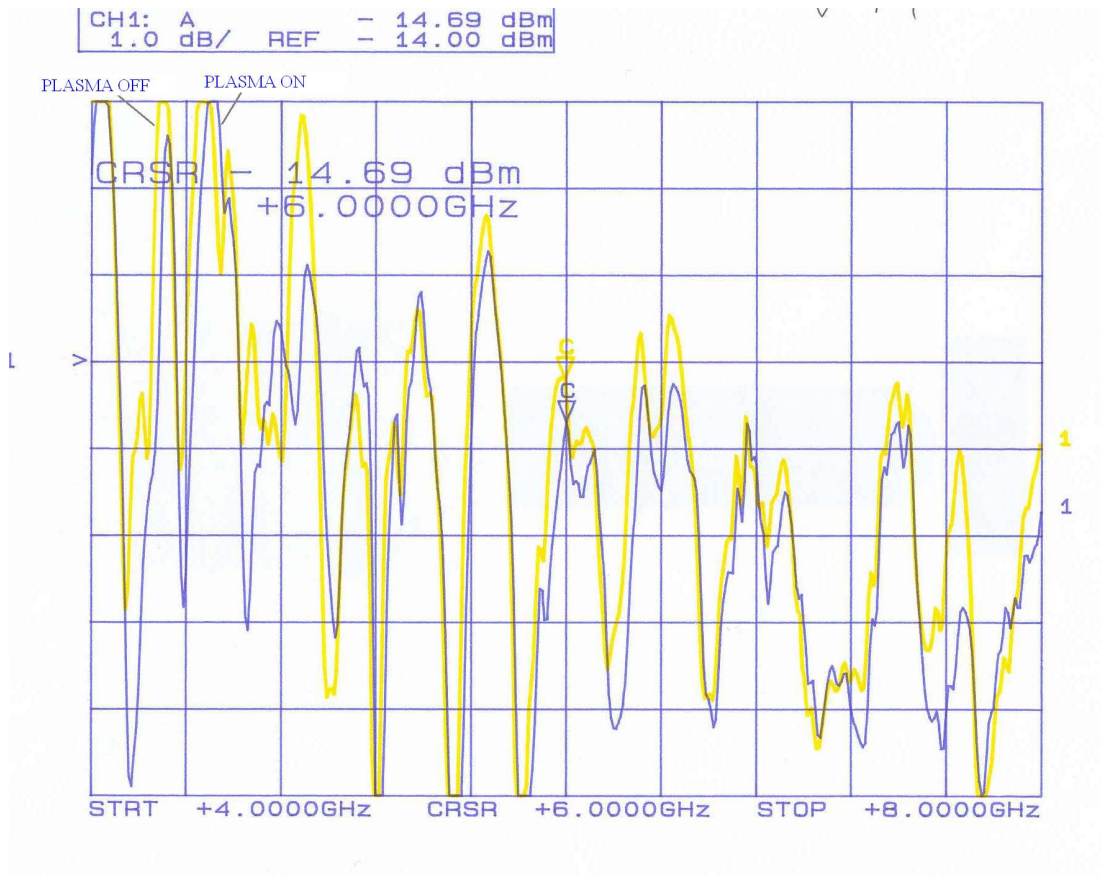
Figure 4.10: Effect of plasma on transmission loss for the frequency range of 4GHz-
8GHz, with scale 1dB/div, for antenna polarization vertical to tube orientation.
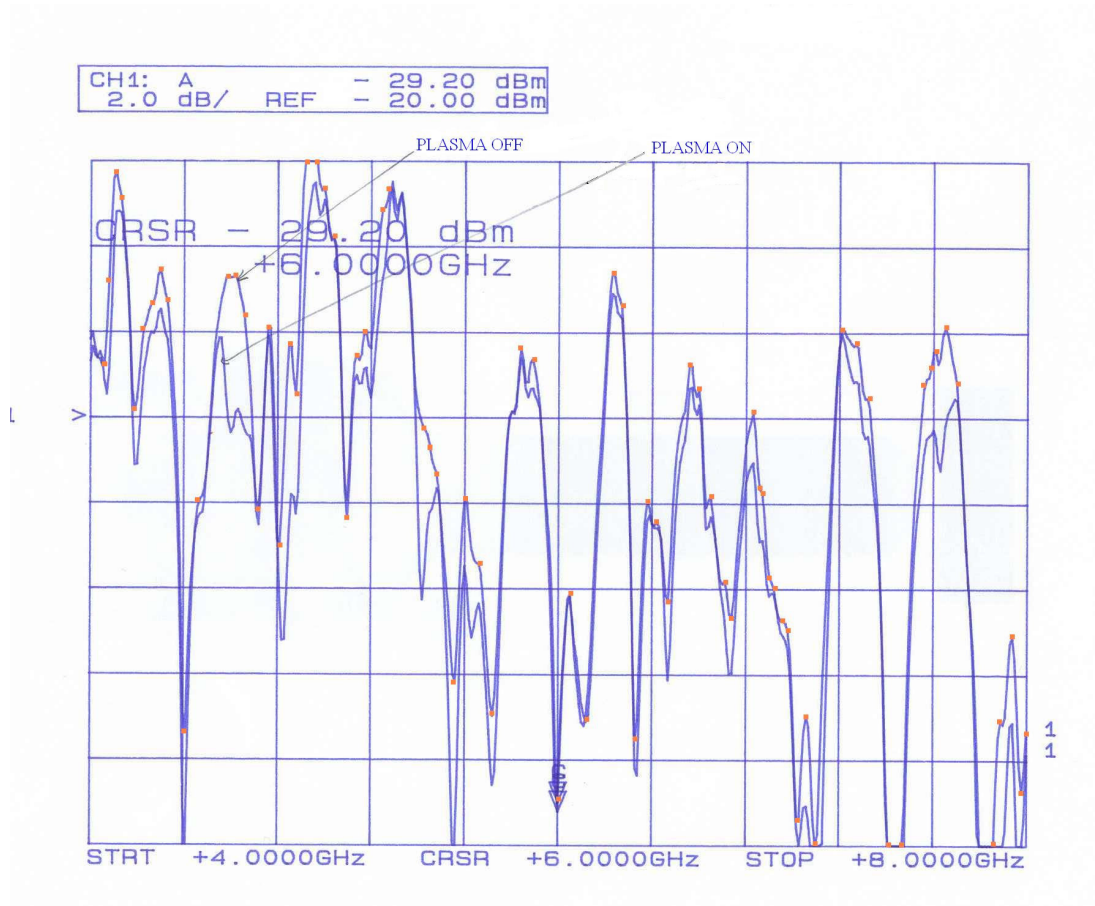
Figure 4.11: Effect of plasma on transmission loss for the frequency range of 4GHz-8GHz, with scale 2dB/div, for antenna polarization parallel to tube orientation.

4.3.2. MICROWAVE REFLECTION EXPERIMENTS

The microwave reflection setup consists of two adjacent horns facing the discharge tube, and a network analyzer that calculates the time domain response from frequency response of the system. Metallic parts of the discharge setup like flanges, valves and electrodes are covered with microwave absorbing materials. Reflection measurement setup is given in Figure 4.12.
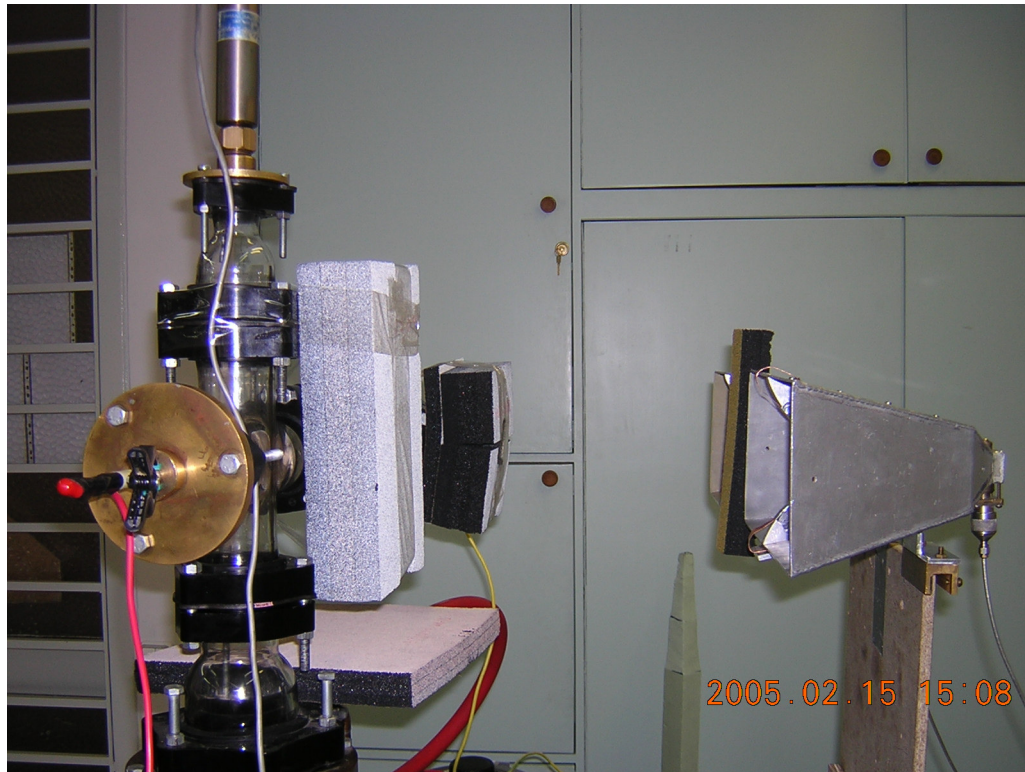
Figure 4.12: Reflection measurement setup, with metallic parts of the setup covered with microwave absorbers

Transforming of data from frequency domain to time domain requires a frequency sweep; the frequency range must be larger to get better time resolution. The largest frequency span that could be obtained with the microwave setup was 1-12 GHz, results of which are given in Figure 4.13. Time resolution of the transformed data is enough to discern the chamber walls as the first two crests in the reflected power graph. Secondary reflection is also discernible as the third crest. The rest of the graph is irrelevant due to continuing multiple reflections and possible reflections from uncovered parts behind the discharge tube.
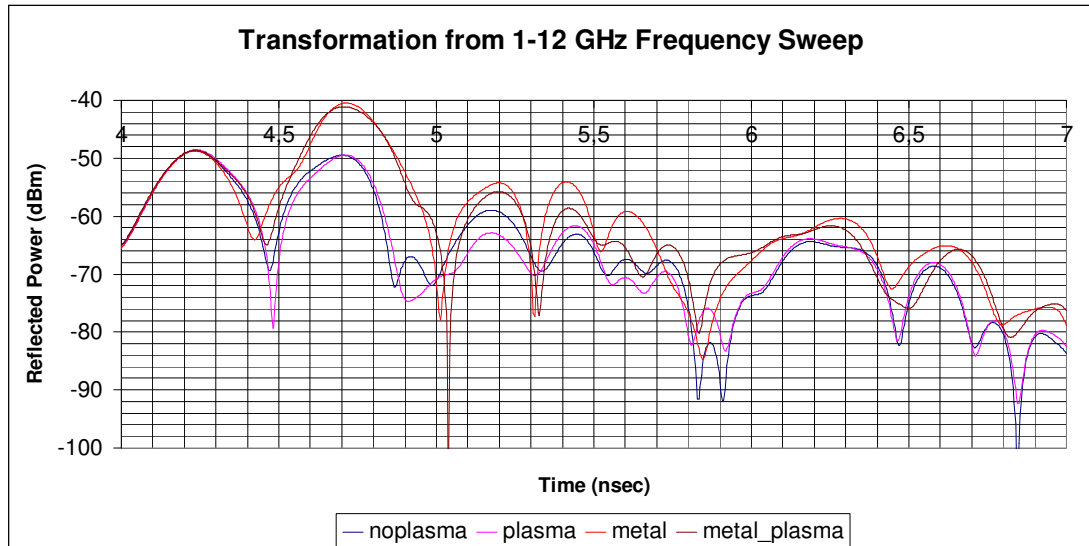
Figure 4.13: Reflection measurements with 1-12GHz frequency sweep

The power absorbing nature of the plasma can be seen in the secondary reflection. The power from secondary reflection is significantly lower when the tube is filled with plasma. The same result is obtained when a metallic plate smaller than the inner radius of the tube is placed behind the discharge tube. Also there is visible delay in the reflections, which is expected due to relative permittivity of the plasma being less than unity. The group velocity of the electromagnetic waves in plasma medium is less than that in free space.

To see the effect of the plasma and plasma frequency more clearly, a second sweep with a frequency range 1-6 GHz is taken. The time domain response of the 1-6 GHz sweep is given in Figure 4.14. The time resolution is not enough to distinguish the front and rear chamber walls in this case. However the secondary reflection is still visible in the graph. The reflection from the tube has visibly increased in this case. The response is as if the electromagnetic waves are faster in plasma, and the secondary reflection is higher than expected. This phenomenon may be due to the dispersive nature of the under-dense plasma, which is very close to the critical density. The frequency response of the system may give such erroneous time domain transformation results due to very high dispersion. The frequency sweep of 1-12 GHz has not shown this phenomenon due to less dispersion for higher frequency components of the signal.
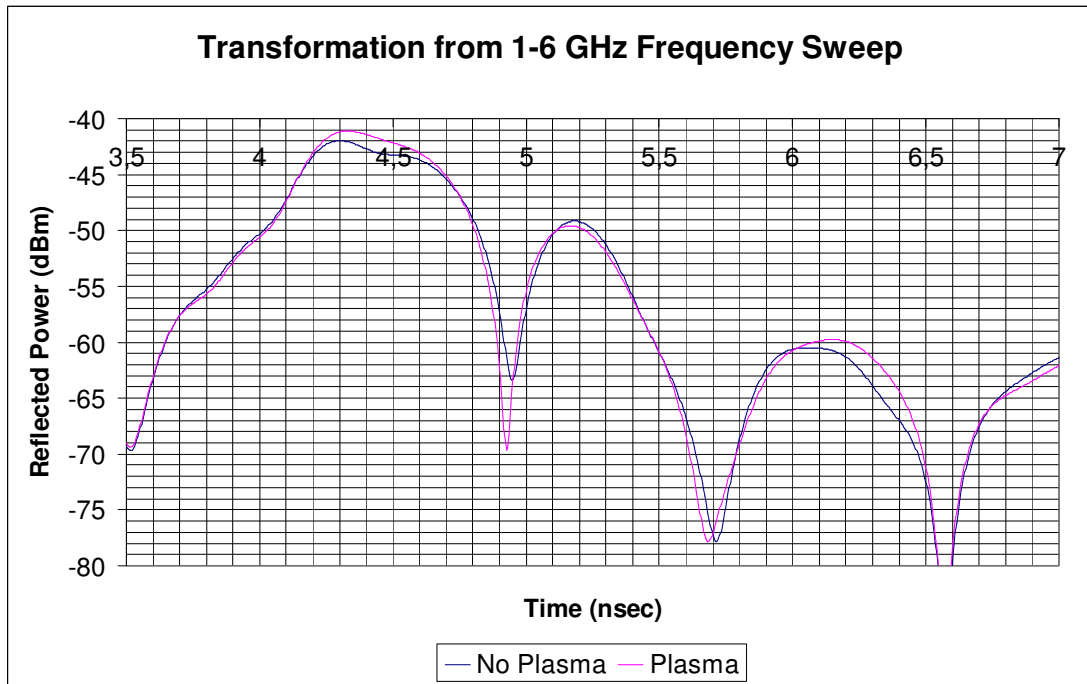
Figure 4.14: Reflection measurements with 1-6GHz frequency sweep

4.3.3. CONCLUSIONS DEDUCED FROM THE EXPERIMENTS

The microwave cut-off and reflection experiments show that a relatively simple DC discharge setup can generate plasma with frequency high enough to cut-off and reflect microwave frequencies. The discharge, however, consumes very high powers if operated with continuous current; DC discharges in pulsed operation mode is much more feasible than continuous operation.

While theoretical calculations show no difference between cut-off and reflection conditions, the plasma frequency requirements for reflection are much stricter than those requirements for cut-off. This discrepancy is due to the fact that the theoretical formulations do not take into account the radial electron density gradient. The plasma closer to the chamber walls is under-dense compared to the calculated plasma frequency. The plasma in the vicinity of the chamber walls is reflecting for lower frequencies only. The under-dense regions and the effect of chamber walls must be taken into account while designing plasma antennas.

CHAPTER 5

APPLICATIONS OF PLASMA MEDIUM IN ANTENNA SYSTEMS

5.1. INTRODUCTION

The equations governing the interaction of plasma medium and electromagnetic waves have been derived in the previous sections. However, making use of plasma medium in antenna systems require study of plasma systems considering the parameters important for the performance of a communication system. The plasma frequency, while enough to determine basic plasma parameters required for interaction, is not enough by itself to analyze the performance of plasma in antenna applications.

In literature various plasma systems are proposed. Due to different needs and performance analysis techniques, the use of plasma can be categorized as reflector, radiator and lens.

5.2. PLASMA REFLECTOR

Using plasma medium as a microwave reflector in radar systems is proposed by Manheimer [1]. In his proposal, Manheimer argued that radar systems with plasma reflectors can replace phased array radars, due to the plasma reflector's agility and broad band performance. Later, the plasma reflector concept is realized and experimented upon extensively [2-7]. The basic experimental setup is given in Figure 5.1.
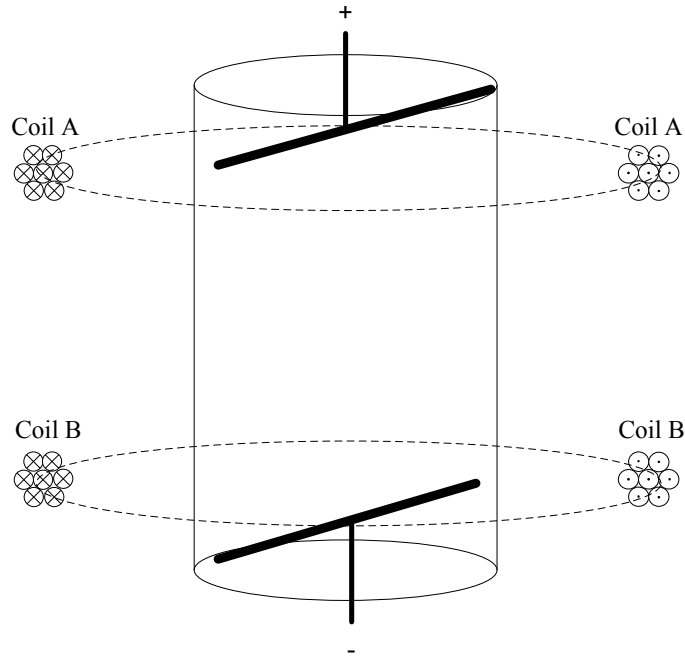
Figure 5.1: The discharge tube [2-6] consists of a hollow cathode and plate anode, with the plasma confined into sheet geometry by the magnetic fields generated by Helmholtz coils (Coil A and Coil B)

In the experimental setup, plasma is shaped into a planar reflector by line-shaped hollow cathodes and magnetic fields generated by Helmholtz coils. Performance of such a system can be evaluated by measuring the microwave noise generated by the plasma and reflector surface quality. The beam steering is achieved by turning off the plasma and reigniting by using different electrode and coil configurations. As the system is proposed as a replacement for phased arrays, agility of this steering scheme must also be considered.

5.2.1. MICROWAVE NOISE EMITTED BY THE PLASMA MIRROR

The problem of determining the amount of microwave noise emitted by the plasma can be considered as a blackbody radiation problem. A blackbody is an entity that absorbs all electromagnetic waves incident upon it. The blackbody emits electromagnetic radiation with spectral energy distribution depending on the blackbody temperature. Thus electromagnetic radiation generated by an object can be calculated from temperature of the object.

The radiation temperature of plasma can be taken as the temperature of free electrons inside the plasma, which is determined from the electron energy. Electron energy of 1 eV corresponds to a plasma temperature of 11600°K. However, the plasma is not a blackbody; microwaves with frequencies lower than plasma frequency are reflected from a critical surface within the plasma. A perfectly reflecting object cannot radiate, thus reflectivity of the plasma medium must be considered. Also the under-dense plasma regions, which have less or no reflectivity, must be taken into consideration. The radiation temperature of the plasma can be formulated as

$$T_r = \eta T_e \qquad\qquad 5.1$$

where T_e is the electron temperature and η is the emissivity of the plasma.

The emissivity of plasma can be calculated from the reflection coefficient of plasma. The plasma is assumed to have a density

$$N(x) = 0 \text{ for } x < 0$$

$$5.2$$

$$N(x) = N_c \alpha x \text{ for } x \geq 0$$

where $\alpha = \dfrac{1}{l}$ is a constant defining the steepness of the electron density gradient of the plasma, l is the length of the under-dense region and N_c is the critical electron density. Thus the plasma is assumed to have a linear density gradient. This assumption is valid for the cases where the under-dense region is very narrow compared to operating wavelength, as in a magnetically confined plasma mirror.

The amplitude reflection coefficient is taken to be

$$|R| \cong e^{\left(-\frac{4kZ}{3\alpha}\right)} \qquad\qquad 5.3$$

where $Z = \dfrac{\nu}{\omega} \ll 1$, ν is the collision frequency, ω is the operating frequency, and $k = \dfrac{\omega}{c}$. Emissivity is found from the reflection coefficient as

$$\eta = 1 - |R|^2 = 1 - e^{\left(-\frac{8\,kZ}{3\,\alpha}\right)} = 1 - e^{\left(-\frac{8\,l\nu}{3\,c}\right)}$$ 5.4

The emissivity for a thickness of 0.5 cm for the under-dense region and collision frequency $\nu = 5 \times 10^8\,Hz$ is $\eta = 0,02198$ [3], and the radiation temperature is $T_r = \eta T_e = 0,02198 \times 11600 = 254,968°K$ from equation 5.1.

In the analysis above, it was assumed that the electron gyro frequency is much smaller than the operating frequency, the density gradient is linear, plasma has planar geometry, and constant collision frequency despite the density gradient [17]. The experiments [2-7] show no significant deviation from the radiation temperature calculated above. Equation 5.4 also shows that radiation temperature increases with the increasing collision frequency.

To verify the radiating temperature figures, a noise measurement was performed in [7]. A high gain antenna is aimed at the plasma reflector at normal incidence from less than 1 meter distance. Figure 5.2 [7] shows the noise measured during 300 μsec pulse generated plasma at 10.5 GHz frequency. The effective temperature of the plasma reflector is calculated to be ~250°K, which agrees with the figure. The noise power is significantly higher in the first 50 μsec, which is due to the turbulent nature of the plasma at that stage.
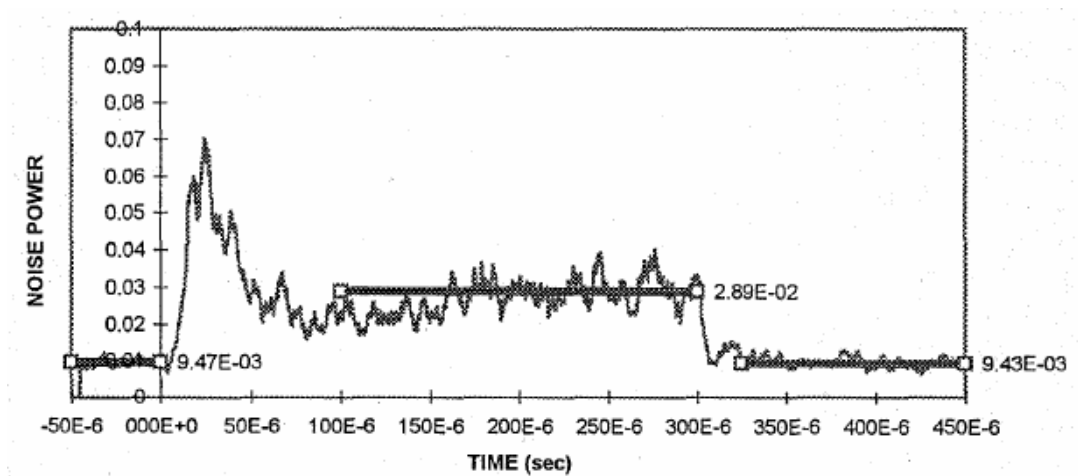

Figure 5.2: Noise power generated by the 300 μsec pulsed discharge plasma mirror at frequency of 10.5 GHz [7]

5.2.2. REFLECTOR SURFACE QUALITY

The reflector surface quality for the proposed plasma reflector can be measured by the smoothness of the surface. However the plasma, being a fluid body, is strongly influenced by diffusion. The unconstrained plasma expands by diffusion and covers the whole plasma chamber. Thus methods must be devised to keep the plasma in a planar geometry.

Confining the plasma by a plane-shaped vessel may be one of the methods. However the plasma suffers from striations at pressures below 1 Torr for a vessel width of 1 cm. The proposed pressure for low radiation temperature and microwave attenuation is below 300 mTorr; plane shaped vessels are not practical at this pressure. The plane shaped vessel also contradicts with the agility requirement.

Magnetic confinement is the method used in plasma reflector experiments [2-7]. Due to decreased collision rates with chamber walls, the striation phenomenon is not observed in this confinement scheme. The confinement criteria for the plasma sheet that ensures reflector surface smoothness is $\omega_{ce} \gg \nu_{en}$ and $\rho_e \ll d$, where ω_{ce} is the electron gyrofrequency, ν_{en} is the electron-neutral collision frequency, ρ_e is the gyroradius and d is the sheet thickness [2]. Derivation of gyrofrequency and gyroradius is given in section 2.7.

For pulse generated plasma, the surface smoothness is also a function of time. The plasma, after the instant of ignition, must settle down to form a stable and smooth reflector surface. This settling period can be determined by interferometer measurements. Such measurements show that the reflector surface contracts during the first 50-100μsec of 300μsec pulse plasma [3].

Another aspect of the surface smoothness problem is the location of critical surface for microwaves with different angles of incidence. The critical density necessary for the reflection is modified as

$$n_{c,eff} = n_c \left(\cos\theta \right)^2 \qquad\qquad 5.5$$

where n_c is the critical density, $n_{c,eff}$ is the effective critical density, and θ is the angle between the incident wave and optical axis, which is normal to the critical surface. Critical density is given in equation 3.14.
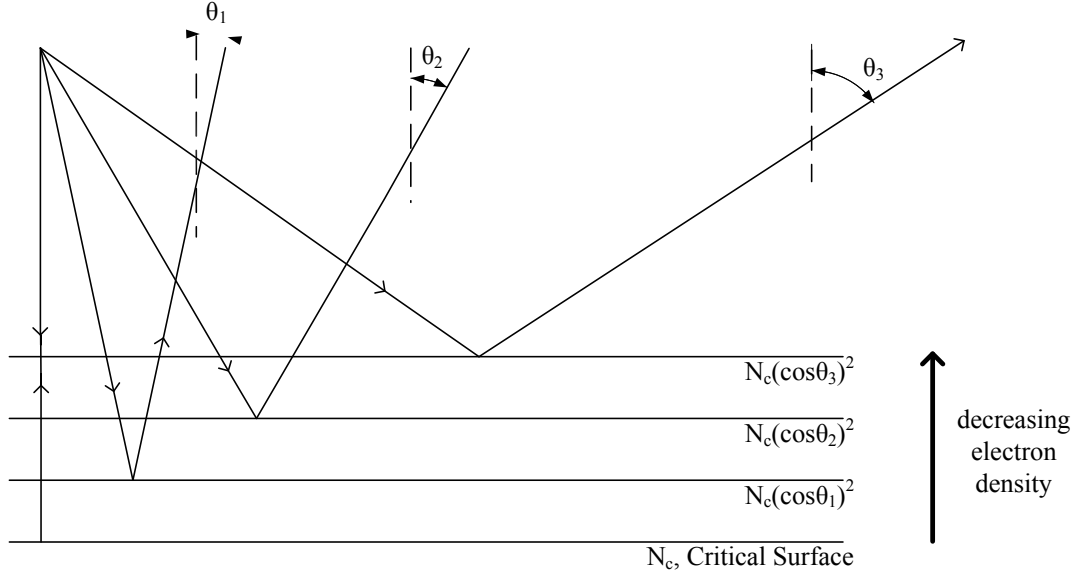
Figure 5.3: Critical surface changes with the angle of incidence.

The modified critical surface expression, as the source antenna is located close to the reflector, may change the reflection pattern significantly if the under-dense region has sufficiently wide span. The modified critical surface expression implies that the main beam of the pattern becomes wider, resulting in lower gain. This effect is, however, quite insignificant for magnetically confined plasma mirrors. Assuming under-dense region width of 0,5 cm, reflector width of 1 meter and source distance of 2 meters, the angle of incidence is

$$\theta = \tan^{-1}\left(\frac{0,5}{2}\right) \cong 14,04° \qquad\qquad 5.6$$

The effective critical density is

$$n_{c,eff} = n_c\left(\cos\theta\right)^2 = n_c \times 0,94 \qquad\qquad 5.7$$

Assuming linear density gradient and under-dense region width of 0,5cm, the effective critical surface is 0,47cm away from the plasma edge. Thus the critical

surface has moved 0,03cm towards the source as a worst case for the dimensions given above.

5.2.3. BEAM STEERING AGILITY

Beam steering is accomplished by changing the orientation of the plasma reflector. The reorientation may be accomplished by tilting the magnetic field or by turning off the plasma and regenerating it by a different electrode combination. Both schemes may be used to steer the beam in both elevation and azimuth.

In order to change the plasma reflector configuration, the initial reflecting plasma must extinguish completely and a new plasma reflector must be initiated with different electrode and magnetic field configuration. Thus, beam steering agility of the plasma reflector is determined by the speed of electrode and magnetic field reconfiguration and by recombination rate of plasma.

The recombination of plasma is a complex process. Recombination rate of electrons and ions roughly depends on the electron energy distribution, electron-ion collision rate, and radiative energy losses. Complete formulation of recombination rates is out of the scope of this thesis. Experimental data shows that plasma reflector can be reconfigured in time scales of 10-20μsec.

5.3.   PLASMA LENS

The dielectric property of plasma is governed by the relation between plasma frequency and electromagnetic wave frequency. For wave frequencies greater than plasma frequency, plasma behaves as a dielectric material, as shown in section 2.6. Due to this behavior, use of plasma as a microwave lens is proposed [10]. The microwave lens system is proposed as a fast beam steering method, although adjustability of plasma parameters suggests that the lens may also be used as an alternative way of agile beam shaping for SDMA and satellite communication schemes. The plasma lens is realized and experimented upon in [10].

The plasma behaves as a lens due to the electron density gradient that naturally occurs in plasma. There is minimum electron density at the chamber walls and the electron density increases towards the center of the chamber. The refractive index of

the plasma changes with the electron density, and electron density is related to plasma frequency by equation 2.27,

$$\omega_{pe} = \left(\frac{N_e q_e^2}{\varepsilon_0 m_e} \right)^{1/2} = 8.94\sqrt{N_e}$$

Graphs of refractive index vs. electron density for several electromagnetic wave frequencies are given in Figure 5.4. As seen in the graph, the refractive index changes with the electron density. Electron density gradient in plasma acts as a lens due to this variation in refractive index as well as the plasma chamber geometry. Ray tracing results for plasma in a cylindrical chamber [10] is given in Figure 5.5. It must be noted that the plasma lens, due to the complex permittivity less than unity, behaves similar to metallic lens. A cylindrical cross section does not collimate the beam in this case; electromagnetic waves are deflected away from higher electron density plasma regions.
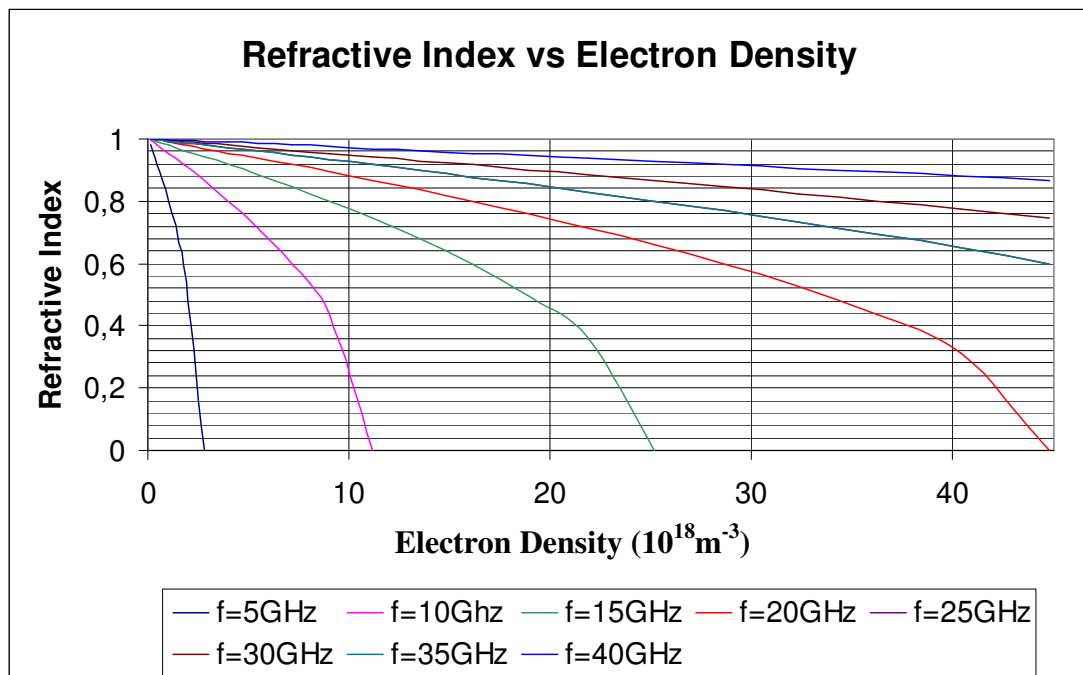
Figure 5.4: Index of refraction vs electron density for several electromagnetic wave frequencies. 10^{18}m^{-3}
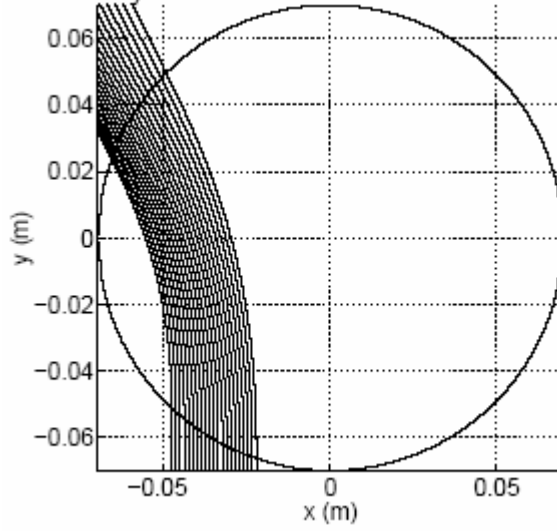
Figure 5.5: Ray trace for electron density of $8 \times 10^{18} / m^3$ at 36GHz wave frequency [10]

The performance of plasma lens can be evaluated by frequency dispersion effects for wide band applications. Contrary to reflectors, where the under-dense plasma regions are very narrow, beam travels large distances through under-dense plasma in a plasma lens compared to its wavelength. Dispersion is unavoidable; however, it can be minimized by selecting appropriate frequency ranges.

5.3.1. FREQUENCY DISPERSION

The dispersion in plasma lenses is caused by the frequency dependent nature of the plasma-wave interaction. The complex permittivity of plasma with negligible collision frequency, as given in equation 2.33, is

$$\varepsilon_r = \varepsilon_r' - j\varepsilon_r'' = \left(1 - \frac{j\sigma}{\varepsilon_0 \omega}\right) = 1 - \frac{j}{\omega \varepsilon_0}\left(-j\frac{N_e q_e^2}{\omega m_e}\right) = 1 - \frac{\omega_p^2}{\omega^2} \qquad 5.8$$

and the index of refraction is

$$n = \left(\mu_r \varepsilon_r\right)^{\frac{1}{2}} \qquad 5.9$$

Assuming relative permeability of the plasma, μ_r to be unity, the index of refraction for the plasma is directly related to plasma frequency, electromagnetic wave

50

frequency and collision frequency. When $\omega_p < \omega$, the plasma behaves as a dielectric with refractive index less than unity.

In order to see the dispersive nature of plasma, a graph of refractive index vs. electromagnetic wave frequency can be obtained for several plasma frequencies, as seen in Figure 5.6. As seen in the graph, as the electromagnetic wave frequency increases the relative permittivity approaches to unity. Also it can be seen from the graph that the rate of change of refractive index with respect to wave frequency is high for frequencies slightly greater than the plasma frequency, which means high dispersion of frequency components of a signal passing through the under-dense plasma. Yet for higher frequencies, the dispersion is not very high. Thus it may be feasible to use a plasma lens for wave frequencies of 10 GHz order. Higher frequencies are also less affected from electron density gradient in plasma, as seen in Figure 5.4.
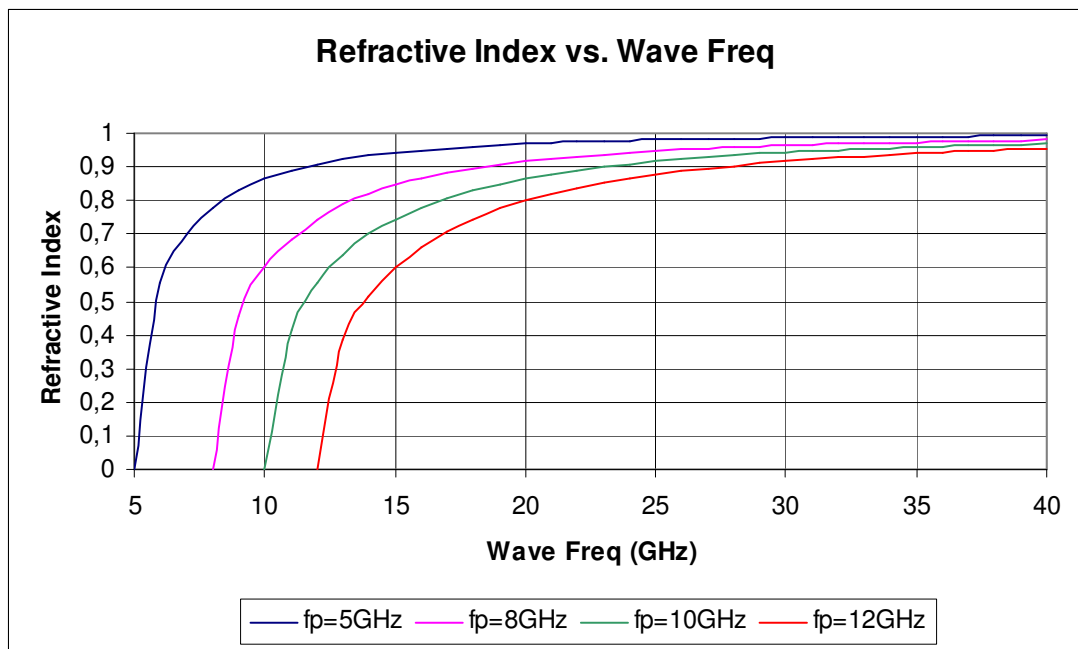

Figure 5.6: Index of refraction vs electromagnetic wave frequency for several plasma frequencies.

5.4. PLASMA RADIATORS

The plasma, being a current carrier, can efficiently radiate and receive electromagnetic waves. The advantage of using plasma as the conductor in an antenna is the ability to make the antenna "disappear" by turning off the plasma. Once turned off, only dielectric tube structure and electrodes remain, which eliminates the mutual coupling and lowers the radar cross section of the antenna significantly. Also due to low plasma frequency, a plasma radiator operating in VHF band is invisible to microwave radars. Thus, the plasma radiators can be used in stealth antenna applications, reconfigurable beam shaping schemes and HF-VHF antennas with low mutual coupling.

Plasma tubes that operate as a radiator may be in many different shapes and plasma can be generated by various methods depending on the intended application. Plasma loops and monopoles are the most common types of plasma radiators. Generation techniques vary from DC discharge to RF surface wave plasmas to laser initiated atmospheric discharges.

5.4.1. ATMOSPHERIC DISCHARGE PLASMA AS AN ANTENNA

The ionization levels required for a plasma column to behave as a good conductor can easily be achieved in atmospheric discharges. However the voltage that is required to form an ionized path through the atmosphere is very high and the discharge path forms in a very random manner. To overcome these obstacles, a laser beam can be used to form a weakly ionized path in the atmosphere, which would guide the discharge along a determined path which is linear.

One of the early experiments [13] shows that such a plasma column generated as explained above can be used as an antenna in VHF frequency band. The required voltage for the initiation of the discharge is around 125kV, however the voltage needed to sustain the discharge is very low, even down to 100V. In the experiment, the laser guided discharge is shaped into a folded monopole, with a copper rod connecting the two plasma columns. The discharge was generated by pulsed current.

The experiment shows that the antenna is not a significant source of noise, and the efficiency and matching characteristics are satisfactory. However due to the

52

extremely high voltage levels and the need for a guiding laser, such an application may not be practical or feasible except for a concept demonstration.

5.4.2. SURFACE WAVE DRIVEN PLASMA AS AN ANTENNA

The common way to generate plasma is to use two electrodes at each end of a tube with electrodes protruding in to the tube. Another method is to use a capacitive coupling mechanism in one end of the tube, with no electrodes on the other end. Such a system has no electrodes in the tube, thus there is no need for metal-dielectric seals which are otherwise required in common tubes for the generation of plasma.

The capacitive coupling generates a surface wave along the plasma column. Such a wave is very similar to the surface wave on a metallic dipole antenna, and the wave propagates near the speed of light for frequencies well below the plasma frequency [11]. The radiation properties of such plasma columns can be determined from surface currents.

The axial current and electron density measurements for a 35 MHz driven plasma column are given in Figure 5.7 [11]. From the figure it can be seen that in order to obtain a plasma column that behaves like a metallic monopole, enough RF power must be supplied to the column so as to make the axial current similar to that of a metallic monopole. Low power results in rapidly decaying current due to low plasma electron density.
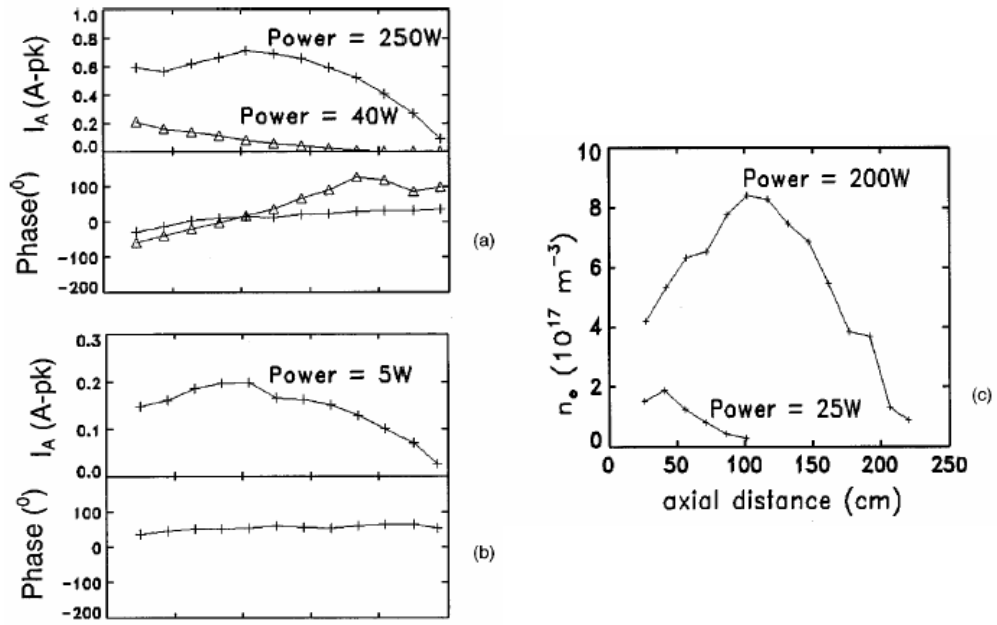
Figure 5.7: On the left axial current amplitude and phase measurements for (a) plasma tube at 35 MHz and (b) copper cylinder, on the right (c) line-integrated electron density for 2430mm plasma tube driven at 30 MHz.

The noise performance of a surface wave driven plasma column radiator is tested in [12]; results of the test are given in Figure 5.8. Two plasma tubes, one driven by 240V, 50Hz AC and other by 140 MHz surface wave excitation, are used as receiving antennas in the frequency range 0-30 MHz, with 21 MHz signal of power 0 dBm launched into the laboratory. A copper antenna is also employed for comparison. The results show that the surface wave driven plasma has noise spectra similar to a metallic antenna. The plasma tube driven by 240V, 50Hz AC has 10-30 dB higher noise across the band.
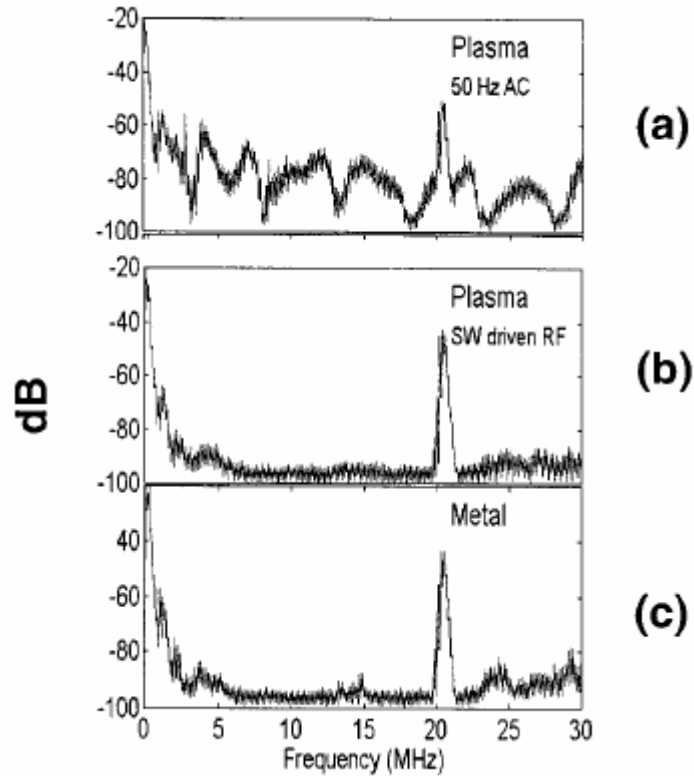
Figure 5.8: The noise spectra received by the two plasma tubes and the copper antenna in 0-30 MHz frequency range, with reference signal at 21 MHz.

The reason for higher noise at lower drive frequency is varying electron density of the plasma. The density variation is measured in [8] for fluorescent tube with reduced mercury content in the gas. The tube contained Argon with rated pressure of 3 Torr and 10^{-4} to 3×10^{-3} Torr mercury, depending on the tube wall temperature. The electron and collision densities calculated from interferometer measurements for the plasma driven by 60 Hz, 120V AC are given in Figure 5.9. The density variation results in generation of noise; the same phenomenon is observed in the initial stages of reflector plasma ignition. The low density plasma is a source for electromagnetic radiation due to low reflectivity of the plasma, as given in section 5.2.1.
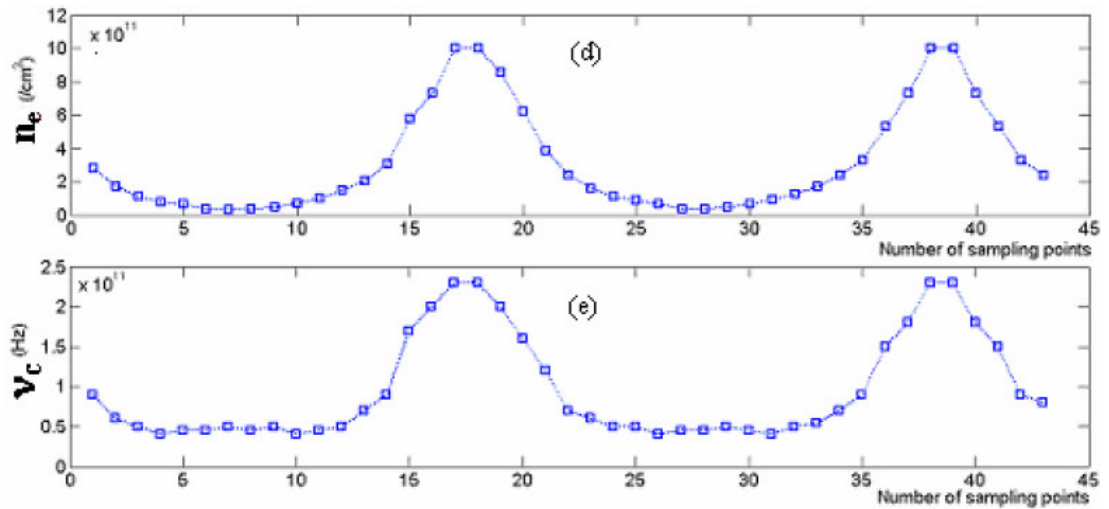
Figure 5.9: Variations in electron density (top) and collision frequency (bottom) for a fluorescent lamp filled with Argon at pressure 3 Torr and 10^{-4} Torr mercury, and driven by 60Hz AC voltage. [8]

In order to reduce the noise generated by the plasma radiator, the plasma must be driven by continuous DC or by RF or pulsed current with repetition time interval much smaller than plasma decay time.

5.5. SEMICONDUCTOR PLASMAS IN ANTENNA APPLICATIONS

Charge carriers in metals and semiconductors behave similar to those in gas plasmas. The medium properties are obviously very different; however, the interaction of electromagnetic waves with charge carriers has very similar properties. The semiconductors having free carrier densities enough to interact with electromagnetic waves are called semiconductor plasmas, due to the analogies between the electromagnetic interaction properties between the gas plasma and semiconductor.

The charge carriers in a crystal structure may be considered as if they are free particles in vacuum, but with different masses and mobility parameters. The masses of charge carriers in the crystal structure are stated in the units of ordinary mass of electron, which is defined as the effective mass. The effective mass term replaces the ordinary mass terms in the equations of interaction of electromagnetic waves with plasma medium. The effective mass concept is valid for low electron energies; most semiconductors have electron energies of the order of 0,01eV. Effective masses for several frequently used semiconductors are given in Table 5-1.

The complex permittivity for the semiconductor plasma can be written as

$$\varepsilon_r' = \varepsilon_r \left[1 - \sum_s \frac{\omega_{ps}^2}{\omega^2 + \frac{1}{\tau_{rs}^2}} \right] \qquad 5.10$$

where the sum is over the free charge carriers and τ_{rs} is the relaxation time for each charge carrier species. Relaxation times have negligible effect for the frequencies on the order of GHz, the $\frac{1}{\tau_{rs}^2}$ term can be neglected altogether. As seen in Table 5-1, the charge carriers have comparable relative masses for most semiconductor types. Due to this fact, we have to take into account both the electrons and holes when calculating the relative dielectric constant and propagation properties.

Table 5-1: Effective masses and dielectric constants for several semiconductors [18]

Material	Electron effective mass	Hole effective mass	Dielectric Constant
Ge	0.2	0.3	16
Si	0.33	0.5	12
InSb	0.013	0.6	18
InAs	0.02	0.4	14.5
InP	0.07	0.4	14
GaSb	0.047	0.5	15
GaAs	0.072	0.5	13

Very high electron densities can be obtained in semiconductors by heating, current injection or optical excitation. The low power requirement, coupled with the elimination of the need for vacuum, makes the semiconductor plasma attractive in many applications. However, the semiconductor plasmas are much more susceptible to frequency dispersions due to the anisotropic nature of the crystal structure and the mass ratio of charge carriers. Exact nature of interaction of electromagnetic waves with crystalline structures is a very extensive topic; inspection of such interaction is out of the scope of this thesis.

An antenna structure utilizing semiconductor plasma is proposed, and the possibility of generating semiconductor plasma dense enough to operate in X-Band is demonstrated theoretically in Chapter 6.

CHAPTER 6

SEMICONDUCTOR PLASMA DIPOLE ARRAY

6.1.   INTRODUCTION

In this chapter, proximity coupled dipole array series fed by a transverse microstrip line is given as a possible application of semiconductor plasma. The dipoles consist of semiconductor plasma, which is generated by optical excitation or current injection. The proximity coupled microstrip dipole array realized on a dielectric substrate is introduced in a practical manner; mathematical modeling is out of the scope of this thesis. A detailed analysis of an ordinary proximity coupled microstrip dipole array can be found in [21].

6.2.   PROXIMITY COUPLED PRINTED DIPOLE ARRAY FED BY A TRANSVERSE MICROSTRIP LINE

There are two possible feeding schemes for the printed antenna arrays. In one method, the elements are fed by a network structure, where each element is connected to the feed network in a parallel configuration. Power is divided by the network structure according to the design requirements. In the other method, series feeding in which the array elements are connected periodically to the transmission line.

The proximity coupled dipole array proposed in this thesis is a series fed linear array structure, where the transmission line is placed between two dielectric layers and radiating elements are printed on the top dielectric layer. The radiators have no contact with the feed line; coupling is controlled by the overlap of radiators and the feed line.

Proximity coupled microstrip dipole configuration has many advantages over other microstrip configurations. Placing the radiating dipole farther from the ground plane leads to greater bandwidth and radiation efficiency, and the feed lines being closer to the ground plane reduces the feed line radiation [20].

A proximity coupled dipole array is given in Figure 6.1. Note that the dipole elements must be placed with an offset relative to the microstrip line; otherwise the fields at the tips of the dipole cancels each other out, resulting in non-radiating dipoles. The maximum coupling occurs when the dipole is placed such that the tip of the dipole coincides with the microstrip line edge.
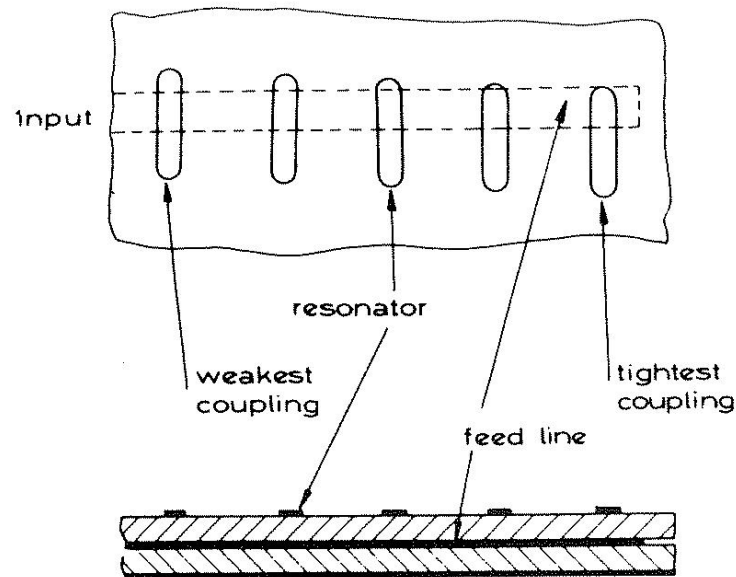
Figure 6.1: Series fed array of proximity coupled microstrip dipoles [25]

The parameters that determine the operating frequency and the beam shape are dipole lengths, dipole offset distances and inter-element spacing. The dipole array can be analyzed by modeling each dipole as a shunt impedance, as given in Figure 6.2. The offset distance and dielectric thickness determine the coupling coefficients between the feed line and the dipoles. Thus, impedance values are determined by the dipole offset distances, upper dielectric layer thickness and dielectric constant. Also the effects of mutual coupling between the dipoles can be included in the impedance values [22].
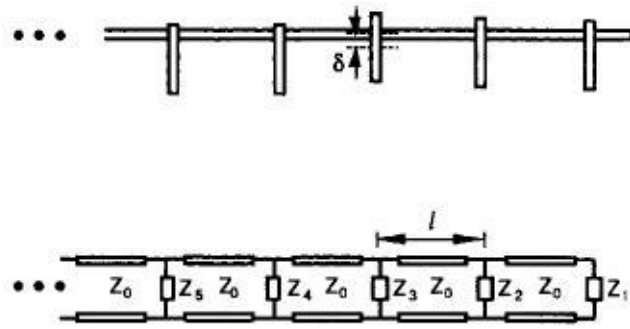
Figure 6.2: Dipole analyses as shunt impedances [23]

6.3.   SEMICONDUCTOR PLASMA DIPOLE GENERATION SCHEME

The proposed semiconductor-based configurable dipole array structures are given in Figure 6.3. The dipoles are created over the semiconductor coating by a predetermined pattern of illumination. The pattern of illumination can be changed to obtain different dipole configurations; a wide variety of antenna radiation characteristics can be obtained. The semiconductor coating on the dielectric layer must be thin in order not to disturb the antenna radiation characteristics very much.
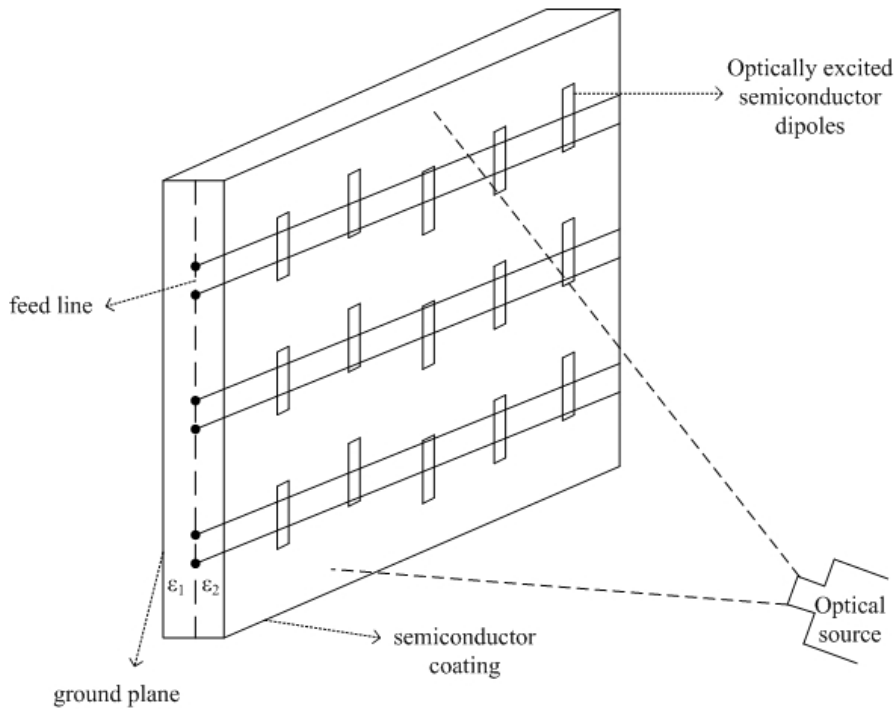
Figure 6.3: Optically excited dipole array configuration

The semiconductor materials have an energy gap between the valance and conduction bands. The energy gap is much smaller than the insulators; thus, thermally excited electrons can have enough energy to cross this gap. Each electron that is excited from the valance band to the conduction band leaves a vacancy in the valance band, which behaves as a positively charged particle with an effective mass depending on the type of material. Thus electron-hole pairs are produced.

While examining the semiconductors for the application proposed above, the correlation between the semiconductor material temperature and electron density in the conduction band must be analyzed. The semiconductor material must behave as an insulator at the operation temperature of the antenna unless it is excited by the laser beam. Also the effects of diffusion and recombination of charge carriers must be considered for the case of optical excitation.

6.3.1. CARRIER CONCENTRATIONS AT THERMAL EQUILIBRIUM

Due to the relatively small energy gap between valance and conduction bands in a semiconductor, electrons can be thermally excited into the conduction band. In order to determine the density of free electrons, the distribution of electrons over the energy levels of a semiconductor structure must be determined; such distribution can be modeled by Fermi-Dirac statistics.

Fermi-Dirac distribution function is stated as

$$f(E) = \frac{1}{1 + e^{\frac{E - E_f}{kT}}}$$

6.1

where $k = 8,62 \times 10^{-5} \frac{eV}{K}$ is the Boltzmann's constant, T is the temperature in units of Kelvin, E is the energy state and E_f is the Fermi level. At energy states equal to Fermi level, the distribution function is

$$f(E_f) = \frac{1}{1 + e^{\frac{E_f - E_f}{kT}}} = \frac{1}{1 + 1} = \frac{1}{2}$$

6.2

An energy state at Fermi level has a probability of 0,5 of being occupied by an electron. The Fermi-Dirac distribution function is given in Figure 6.4.
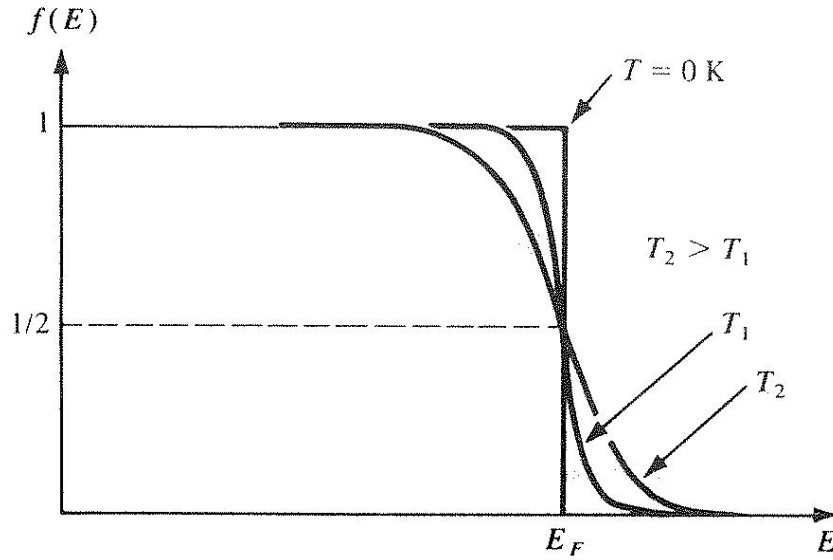
Figure 6.4: Fermi-Dirac distribution function [27]

In intrinsic semiconductors such as Silicon (Si) or Germanium (Ge), the density of electrons and holes must be equal to each other. Due to the odd symmetry of the Fermi-Dirac distribution function, Fermi level in a pure intrinsic semiconductor is located in the middle of the band gap, making the electron and hole concentrations equal.

The Fermi-Dirac distribution function can be used to calculate the electron and hole densities in a semiconductor. The concentration of electrons in the conduction band, for example, can be determined from

$$n_0 = \int_{Ec}^{\infty} f(E)N(E)dE \qquad\qquad 6.3$$

where N(E)dE is the density of states in the energy range dE [27]. The integration limits are from the bottom energy level of the conduction band to the infinity. Although the conduction band does not extend to infinite energy, the above integral is still valid; the Fermi distribution becomes very small for large values of E.

Instead of solving the integral in equation 6.3, we may express the distribution of electrons on the energy levels of the conduction band as if all electrons are at the bottom energy level of the conduction band, E_c, with an effective density of states N_c. The density of electrons in the conduction band becomes

$$n_0 = N_c f(E_c) \tag{6.4}$$

where $f(E_c)$ can be simplified as

$$f(E_c) = \frac{1}{1 + e^{\frac{(E_c - E_f)}{kT}}} \approx e^{-\frac{(E_c - E_f)}{kT}} \tag{6.5}$$

Since kT at room temperature is 0,026 eV, the above approximation is valid.

The effective density of states N_c is given in [27] as

$$N_c = 2\left(\frac{2\pi m_n^* kT}{h^2}\right)^{\frac{3}{2}} \tag{6.6}$$

where m_n^* is the effective mass of electrons in the semiconductor of interest, k is the Boltzmann's Constant, h is the Planck Constant, and T is the temperature of the semiconductor of interest in units of Kelvin. Using equations 6.1 and 6.6, electron densities for different semiconductors at various temperatures can be calculated. Also the values of N_c at 300°K for many semiconductors are tabulated, and formulations that directly relate the effective density of states with temperature are derived in literature [28].

The same formulas hold for the hole density in the valance band;

$$p_0 = N_v[1 - f(E_v)] \approx N_v e^{-\frac{(E_f - E_v)}{kT}} \tag{6.7}$$

$$N_v = 2\left(\frac{2\pi m_p^* kT}{h^2}\right)^{\frac{3}{2}} \tag{6.8}$$

where p_0 is the hole density in the valance band, m_p^* is the effective mass of holes, E_v is the upper energy level of the valance band and N_v is the effective density of states for holes in the valance band.

6.3.2. OPTICAL GENERATION OF EXCESS CARRIERS IN SEMICONDUCTORS

The electron-hole pairs can also be introduced into the semiconductor by optical excitation of electrons. An incoming photon must have energy

$$h\nu \geq \Delta E \qquad\qquad 6.9$$

in order to excite an electron, where ΔE is the energy gap between the valance and the conduction bands, ν is the photon frequency, and h is the Planck's Constant. When a beam of photons with such energies falls on a semiconductor, a certain amount of photon absorption occurs. The amount of absorption is determined by the material properties and thickness of the semiconductor material under consideration.

An optical absorption coefficient α can be calculated for each semiconductor type, and the amount of photons absorbed by a semiconductor specimen can be expressed as

$$P_A = P_0\left(1 - e^{-\alpha l}\right) \qquad\qquad 6.10$$

where P_A is the number of absorbed photons, P_0 is the number of incident photons, and l is the distance the beam travels through the semiconductor. As the absorption coefficient α depends on the wavelength of the photons, the above equation is valid only for a monochromatic beam. Formulations that relate optical absorption coefficient α to photon energies are derived for many semiconductor materials in literature [28].

6.3.3. STEADY STATE DIFFUSION AND RECOMBINATION OF CARRIERS

The charge carriers in a semiconductor can be separated according to their origin into two as charge carriers existing in a semiconductor due to its temperature are intrinsic carriers [27]. A semiconductor material which is not excited by any other means has intrinsic carriers for temperatures above 0°K, as explained in section 6.3.1. If the semiconductor material is excited further by optical or electrical means, excess carriers are generated.

Excess carriers generated in a region of a semiconductor diffuse towards the regions with less carrier density. The rate of change of carrier densities can be linked to diffusion and recombination for the case of electrons as

$$\frac{\partial \delta n}{\partial t} = D_n \frac{\partial^2 \delta n}{\partial x^2} - \frac{\delta n}{\tau_n} \qquad 6.11$$

where δn is the excess electron density (carriers introduced by optical excitation in our case), D_n is the diffusion coefficient, and τ_n is the recombination lifetime. Equation 6.11 tells us that the rate of change of excess carriers at a point in the semiconductor is given by the diffusion and recombination of excess carriers.

Equation 6.11 is true for a one dimensional case, where excess charge carriers are generated at one end of a long semiconductor bar and diffuses towards the other end. Although our diffusion problem is three dimensional, the implications of the one-dimensional case can be used for three-dimensional case without the loss of generality.

In steady state, the density of excess carriers are maintained; equation 6.11 becomes

$$D_n \frac{\partial^2 \delta n}{\partial x^2} = \frac{\delta n}{\tau_n} \Rightarrow \frac{\partial^2 \delta n}{\partial x^2} = \frac{\delta n}{D_n \tau_n} = \frac{\delta n}{L_n^2} \qquad 6.12$$

where L_n is the electron diffusion length. The differential equation in equation 6.12 has a solution in the form

$$\delta n(x) = C_1 e^{\frac{x}{L_n}} + C_2 e^{-\frac{x}{L_n}} \qquad 6.13$$

The constants can be evaluated using the boundary conditions. For a very long semiconductor bar, as $x \to \infty$, the excess carrier density must reduce to zero, making $C_1 = 0$. At x=0 excess carriers are injected into the semiconductor; second boundary condition is the density of excess carriers at the injection point. From the solution, it can be noticed that the excess carrier density drops exponentially with the distance from the region of excitation to zero.

For a very thin specimen of semiconductor, when excitation is homogeneous over the surface, we may disregard the diffusion and write the steady state excess carrier density as [27]

$$\delta n = g_{op} \tau_n \qquad\qquad 6.14$$

where g_{op} is the optical generation rate. Thus it can be clearly seen that the excess carrier density is strongly affected by the carrier lifetime. Optical generation rate can be determined from the photon energy, absorption coefficient and power of the light source.

6.3.4. DETERMINING THE SEMICONDUCTOR MATERIAL AND ILLUMINATION POWER

From the above analysis, the important factors in determining the semiconductor suitable for our purposes are the diffusion length, carrier lifetime, optical absorption coefficient, band gap, and thermal generation of carriers. As an example, Silicon is chosen as the semiconductor to be used.

As semiconductors usually have quite high dielectric constants compared to the dielectric materials generally used in microstrip antennas, the semiconductor material on the top layer must be as thin as possible in order not to disturb the radiation characteristics of the antenna. The thin semiconductor materials must be able to absorb a high percentage of the light incident upon them in order to increase the efficiency of excitation. Thus the optical absorption coefficients are of importance. The band gap determines the wavelength of optical excitation, and the optical absorption coefficient depends on the selected wavelength.

For Silicon, the optical absorption coefficient is given in the graph in Figure 6.5. The energy gap of pure Silicon is 1,12eV at 300°K temperature, requiring photons with energies higher than 1,12eV for optical excitation. Photons' having higher energy does not increase the excess carrier concentration; each photon generates one electron-hole pair. For this reason, the light source should be chosen so that the photon energy is slightly greater than energy gap. The optical absorption coefficient is very high for photon energies larger than energy gap. 1,5eV photon energy corresponds to an absorption coefficient about 10^3cm^{-1} for silicon. For a silicon layer

of 50μm $\left(50 \times 10^{-4}\,cm\right)$ thickness, the percentage of absorbed photons can be calculated from equation 6.10 as

$$P_A = P_0\left(1 - e^{-10^3 \times 50 \times 10^{-4}}\right) = P_0\left(1 - 0{,}0067\right) = 0{,}9932 P_0 \qquad 6.15$$

From the above result, we may conclude that thin semiconductor coating does not cause any problem from the point of optical excitation.
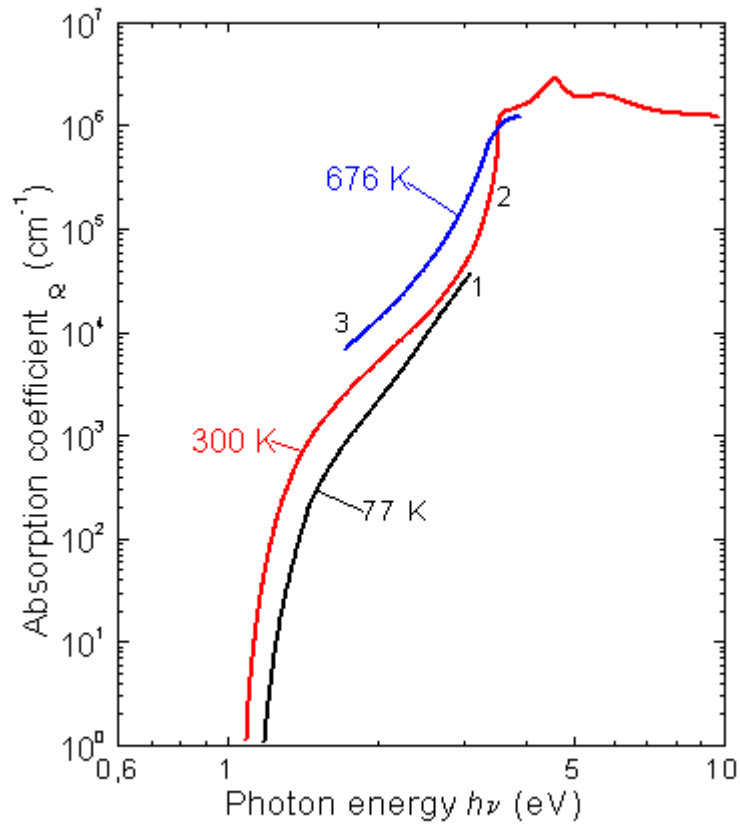
Figure 6.5: Optical absorption coefficient vs. photon energy for silicon at different temperatures [28]

The illumination power required for the operation depends on the carrier lifetime, band gap of the semiconductors and frequency of operation of the antenna. Short carrier lifetime implies that the excess electron-hole pairs generated by the optical excitation recombine rapidly. In order to obtain a required electron-hole density, very

68

large number of photons, thus greater amount of power is required for shorter excess carrier lifetimes. If we continue with the example of Silicon, we have 1,5eV photon energy, and carrier lifetime asymptotically approach to 1ms as silicon purity increases, as seen in Figure 6.6. In this case, the required number of photons for an excess carrier density δn can be calculated from equation 6.14 as

$$g_{op} = \frac{\delta n}{\tau_n} = \delta n \times 10^3 \; photons \cdot \sec^{-1} \qquad\qquad 6.16$$

and the required power is

$$P_o = E_p \times g_{op} = \delta n \times 10^3 \times 1,5eV \cdot \sec^{-1} \cdot cm^{-3}$$
$$= \delta n \times 10^3 \times 1,5 \times 1,60217653 \times 10^{-19} \; J \cdot \sec^{-1} \cdot cm^{-3}$$

$$6.17$$

where δn is in cm^{-3}, E_p is the energy of a single photon, and P_0 is the optical power required to generate the required excess carriers in 1cm^{-3} unit volume.
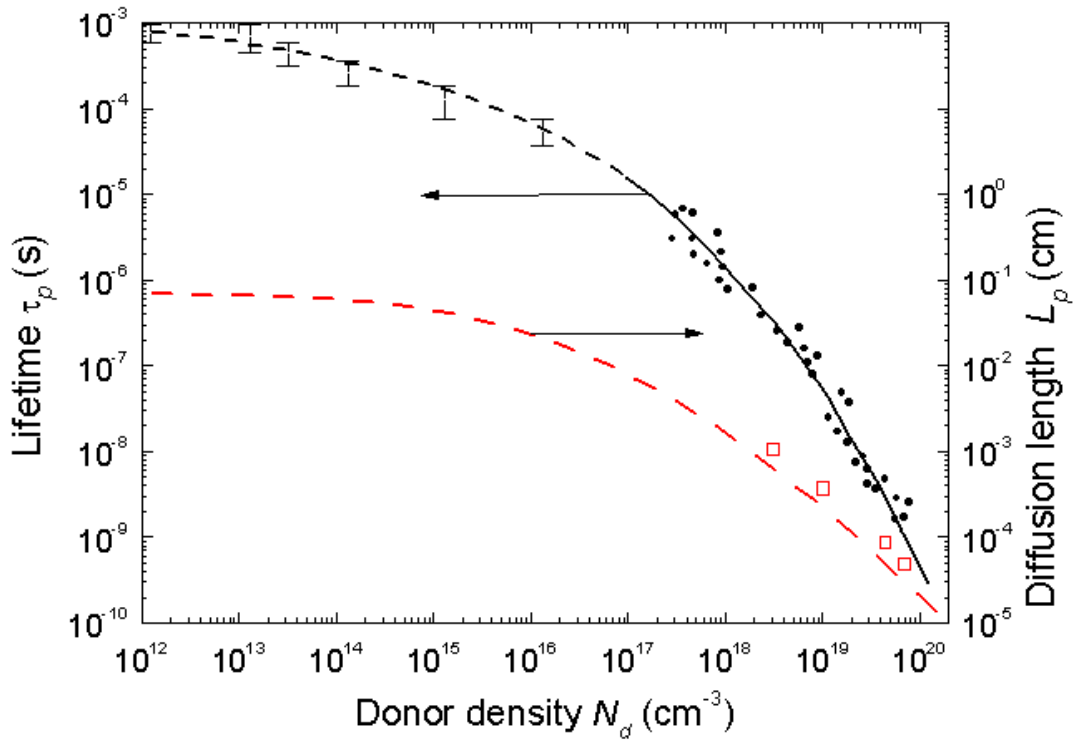

Figure 6.6: Carrier lifetime (black curve) and diffusion length (red curve) vs donor density for silicon [28]

For an operating frequency of 10GHz, the required electron and hole density can be calculated from equation 5.10.

$$\varepsilon_r' = \varepsilon_r \left[1 - \sum_s \frac{\omega_{ps}^2}{\omega^2 + \frac{1}{\tau_{rs}^2}} \right] \leq 0 \Rightarrow \omega^2 \leq \sum_s \omega_{ps}^2 \qquad 6.18$$

and from the plasma frequency expression in equation 2.25,

$$\omega^2 \leq \frac{n_e q^2}{m_e^* \varepsilon_0} + \frac{n_p q^2}{m_p^* \varepsilon_0} = \frac{n_c q^2}{\varepsilon_0} \left(\frac{1}{m_e^*} + \frac{1}{m_p^*} \right) \qquad 6.19$$

where $n_e = n_p = n_c$ is the carrier density for electrons and holes in pure silicon.

For silicon, $m_e^* = 0{,}33 m_e$ is the effective mass of the electron and $m_p^* = 0{,}5 m_e$ is the effective mass of the hole. Thus, required carrier density for electrons and holes is

$$n_c \geq \frac{\omega^2 \varepsilon_0}{q^2} \left(\frac{0{,}33 + 0{,}5}{0{,}33 \times 0{,}5 m_e} \right)^{-1}$$
$$= \frac{10^{20} \times 8{,}8541878 \times 10^{-12}}{\left(1{,}60217653 \times 10^{-19} \right)^2} \left(\frac{0{,}83}{0{,}165 \times 9{,}1093826 \times 10^{-31}} \right)^{-1} \qquad 6.20$$

$$\Rightarrow n_c \geq 0{,}247 \times 10^{18} \cdot m^{-3} = 0{,}247 \times 10^{12} \cdot cm^{-3}$$

where

$$q = 1{,}60217653 \times 10^{-19} \text{ Coulomb}$$

$$m_e = 9{,}1093826 \times 10^{-31} \text{ kg}$$

$$\varepsilon_0 = 8{,}8541878 \times 10^{-12} \text{ Farad/meter}$$

The intrinsic (caused by semiconductor temperature level) carrier density of Silicon at 300°K is around $10^{10} cm^{-3}$, thus we can disregard the intrinsic carriers in the calculations of required optical power. From equation 6.17, inserting the required excess carrier density into the equation, we get

70

$$P_o \geq \delta n \times 10^3 \times 1,5 \times 1,60217653 \times 10^{-19} J \cdot \sec^{-1} \cdot cm^{-3}$$
$$= 0,247 \times 10^{12} \times 10^3 \times 1,5 \times 1,60217635 \times 10^{-19}$$
$$\Rightarrow P_o \geq 0,594 \times 10^{-4} Watt \cdot cm^{-3}$$

<div align="right">6.21</div>

A single semiconductor dipole with dimensions $5cm \times 0,1cm \times 50\mu m$ requires a power of

$$P_{dip} = 0,594 \times 10^{-4} \times 5 \times 0,1 \times 50 \times 10^{-4} = 14,85 \times 10^{-8} Watt$$

or, in units of dBm,

$$P_{dip} = 10 \log\left(14,85 \times 10^{-5} mWatt\right) = -38,28 dBm$$

Thus, a very simple optical source is able to generate the excess carriers required for X-Band operation of a large array.

For thicker coating, assuming the thickness is not comparable to diffusion length, the power requirement is calculated using the same formulation. For the same dipole size with $100\mu m$ thickness, the required optical power per dipole is

$$P_{dip} = 0,594 \times 10^{-4} \times 5 \times 0,1 \times 100 \times 10^{-4} = 29,7 \times 10^{-8} Watt$$

or, in units of dBm,

$$P_{dip} = 10 \log\left(14,85 \times 10^{-5} mWatt\right) = -35,27 dBm$$

In the discussion above, we have disregarded diffusion of carriers. The average diffusion length of 10^{-1} cm. from Figure 6.6 implies that diffusion can distort the dipole patterns imprinted by optical excitation. In order to avoid diffusion of excess carriers, continuous semiconductor coating over the surface should be avoided. Semiconductor dipoles can be placed over the surface in a patched layout as given in Figure 6.7; those dipoles that are necessary for a specific configuration can be illuminated while others are shadowed by the optical projection system, effectively making them non-interacting with the electromagnetic waves.
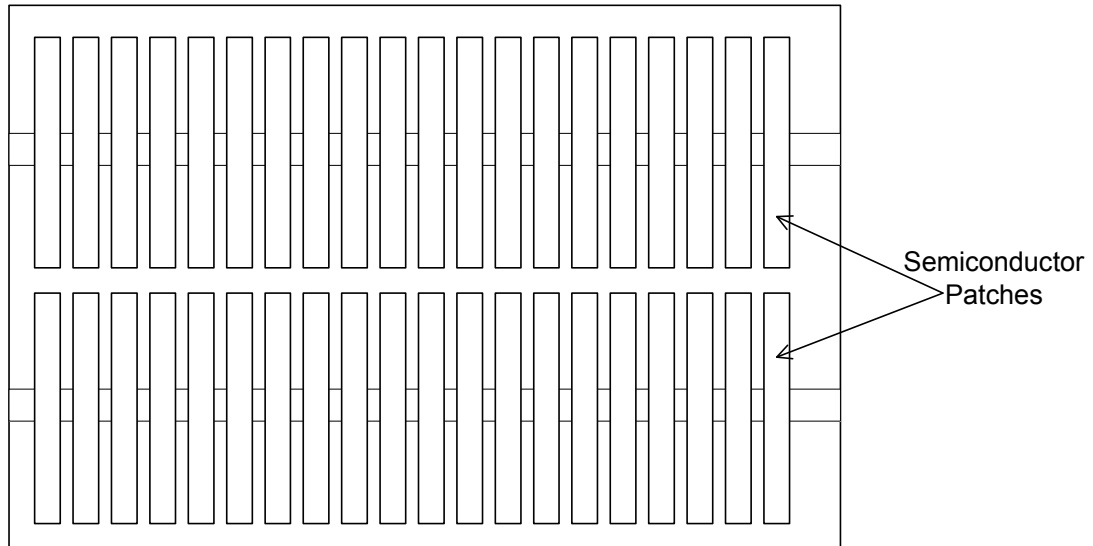
Figure 6.7: Patched semiconductor coating to prevent distortion of dipole geometry by diffusion of carriers

For the semiconductor materials with short carrier lifetime, the diffusion length is also significantly lower. In that case, a continuous semiconductor coating may be feasible. However, the effect of reduced carrier density at the dipole edges on the radiation and impedance characteristics of dipoles must be considered. Also the short carrier lifetime may give lower excess carrier density towards the bottom surface of the dipoles, since the excess carriers are generated on the top surface of the semiconductor by optical excitation.

The carrier lifetime of 1ms deteriorate due to impurities in the semiconductor structure. It may even be desired to give the semiconductor a shorter carrier lifetime in order to be able to reconfigure the antenna layout in a very short time scale. From the discussion above, it can be seen that even for a carrier lifetime of $1\mu sec$, the required power to obtain the necessary carrier density is still less than $100\,mWatt\cdot cm^{-3}$ for the example of silicon. For semiconductor materials with larger energy gap the required power is still affordable, lower than $1\,Watt\cdot cm^{-3}$. For a single dipole the required energy is on the order of mWatt. A single source of illumination with a simple optical mask can produce the required array pattern on the semiconductor coating.

The low optical power requirement for the dipole excitation demands that the antenna must be kept away from light and heat sources. Sunlight, for example, would render the antenna useless by introducing excess carriers to the whole antenna surface. Antenna must be kept in a radom, which is opaque to wavelength of excitation.

The relationship between the supplied power and cut-off frequency in semiconductor is similar to that in gas plasma. As can be seen from equations 6.20 and 6.21, doubling the frequency of operation requires 4 times more power. However, due to the very low power levels required for X-band operation, it can be asserted that operation in the millimeter wave range is possible and feasible.

Due to recombination, some amount of the energy supplied by the excitation source will be dissipated as heat, increasing the semiconductor temperature. At this point the increase in the carrier density with increasing temperature must be calculated, for if the carrier density increases beyond the critical density for the operation frequency, the proposed antenna structure will malfunction. From the calculations of equation 6.21, however, it can be seen that the heat energy supplied by the optical source is far from increasing the temperature.

6.4. RECONFIGURABLE ARRAY STRUCTURE

By changing the dipole location relative to the microstrip feed line and adjusting inter-element spacing, a wide range of beam shaping schemes can be obtained. Different coupling coefficients for each dipole can be obtained, resulting in different current amplitude and phase distributions on the dipoles. Thus, reconfigurable dipole positions would have agility comparable to that of phased arrays. Moreover, the frequency of operation and beam shape can be changed, which may be used as a jammer rejection mechanism in military radar applications.

The dipoles can be reconfigured in a very short time by changing the illumination pattern on the semiconductor coating. Pulsed operation in different frequency bands can be achieved by changing the projection pattern at each pulse interval.

CHAPTER 7

CONCLUSIONS

Throughout this thesis, theory of interaction of electromagnetic waves with plasmas is introduced. The main parameter that governs the interaction is the ratio of electromagnetic wave frequency ω to plasma frequency ω_p, which is in turn related to electron number density of plasma. There are roughly two possible cases, $\omega < \omega_p$ where the plasma acts as a reflector and $\omega > \omega_p$ where plasma acts as a dielectric with relative permittivity less than unity. Each of these cases may be modified by varying other plasma parameters like collision frequency and gyrofrequency.

Since DC discharge is the method chosen for plasma generation, the relation between plasma electron density and current density passing through the plasma is derived. Properties of the cathode sheath region of discharge are used to determine the electron density-current density relation. The formulations are solved for Argon plasma, and it is found out that generating plasma with frequency of 9 GHz is possible with a simple setup. Through the experiments on the interaction of plasma with microwaves, the formulations are verified to a degree.

The experiments on the interaction of plasma and microwaves show that generating plasma with high plasma frequency and continuous current flow is no easy task. The density of DC discharge is inherently limited by the break-down of the plasma, and the power consumption is very high for continuous discharge. The pulsed discharge offers a solution for the power consumption problem; however, the plasma is turbulent during the initial stages of the pulse. Thus, continuous DC discharge gas plasma is not suitable for mm wave operation.

Investigations on the semiconductor plasma show that a wide range of plasma frequencies can be obtained with very low excitation energies. By simply changing the excitation pattern over a bulk semiconductor coating, beam shape and frequency of operation of a semiconductor-coated microstrip antenna can be reconfigured very

quickly. However, the semiconductor surfaces must be kept away form any other source of illumination.

7.1.   FUTURE WORK

Different plasma generation techniques have different advantages that may be suitable for certain applications. While DC discharge is studied in this thesis, generation of plasma with RF discharge is also possible and studied in various institutes. Generation of such plasma and its applications in antenna structures may be a possible course of study.

Being able to reconfigure the antenna structure according to the requirements of the moment in a short time scale may find great use in antenna applications. Plasma medium offers this ability of fast reconfiguration. In future, studies focused on reconfiguration schemes may be conducted for various antenna systems, including phased array and ultra wide band structures.

Magnetized plasma offers a wide variety of configuration schemes. Electron density can be locally enhanced by laser or electron beams, and due to the confinement by the magnetic field, the electrons will not diffuse into the surrounding regions. Such local enhancements may prove to be useful for beam shaping applications; thus, magnetized plasma should be studied in detail.

Semiconductor plasma may have a wider range of applications in antenna structures, since there is no need for vacuum and material with very different properties can be designed. An antenna structure utilizing semiconductor plasma has been proposed in Chapter 6. Semiconductor plasma generation techniques and behavior of different semiconductor material must be studied before a design project can be undertaken.

Realization of such applications of semiconductor plasma requires studies on the generation and behavior of semiconductor plasma of different substrate materials. Each semiconductor substrate has different dielectric properties, and doping significantly changes the behavior of semiconductor materials. Also there are many semiconductor plasma generation techniques, optical excitation being one of them.

Current injection is also another semiconductor plasma generation technique, which has to be studied in detail. Generation and control of semiconductor plasma by current injection may prove a better choice for mass production of antenna systems. Reconfigurable antenna elements by electronic control may be used in millimeter wave array applications; such an array can be built on a single chip by semiconductor fabrication techniques.

REFERENCES

1. Manheimer W.M., "Plasma Reflectors for Electronic Beam Steering in Radar Systems", IEEE Transactions on Plasma Science, Vol. 19, No. 6, pp.1228-1234, December 1991

2. Robson A.E., Morgan R.L., Meger R.A., "Demonstration of a Plasma Mirror for Microwaves", IEEE Transactions on Plasma Science, Vol. 20, No. 6, pp.1036-1040, December 1992

3. Mathew J., Meger R.A., Gregor J.A., Pechacek R.E., Fernsler R.F., Manheimer W.M., "Electronically Steerable Plasma Mirror for Radar Applications", International RADAR Conference, 1995., Proceedings IEEE, pp.742-747

4. Mathew J., "Electronically Steerable Plasma Mirror Based Radar-Concepts and Characteristics", IEEE AES Systems Magazine, pp.38-44, October 1996

5. Mathew J., Meger R.A., Gregor J.A., Murphy D.P., Pechacek R.E., Fernsler R.F., Manheimer W.M., "Electronically Steerable Plasma Mirror", Phased Array Systems and Technology, 1996., IEEE Symposium on, pp.58-62

6. Mathew J., Meger R.A., Fernsler R.F., Murphy D.P., Pechacek R.E., Manheimer W.M., "Electronically Steerable Plasma Mirror Based Radar Antenna", 10th International Conference on Antennas and Propagation, 14-17 April 1997, Conference Publication No. 436, pp1469-1473

7. Meger R.A., Fernsler R.F., Gregor J.A., Manheimer W.M., Mathew J., Murphy D.P., Myers M.C., Pechacek R.E.; "X-Band Microwave Beam Steering Using a Plasma Mirror", Aerospace Conference, 1997., Proceedings, IEEE, vol.4, pp.49-56

8. Howlader M.K., Yang Y., Roth J.R.; "Time-Resolved Measurement of Electron Number Density and Collision Frequency for a Fluorescent Lamp Plasma Using Microwave Diagnostics", Plasma Science, IEEE Transactions on, vol.33, Issue 3, pp.1093-1099, June 2005

9. Laroussi M., Roth J.R., "Numarical Calculation of the Reflection, Absorption, and Transmission of Microwaves by a Nonuniform Plasma Slab" IEEE Transactions on Plasma Science, Vol. 21, No. 4, pp. 366-372, August 1993

10. Linardakis P., Borg G.G., Harris J.H., "A Plasma Lens for Microwave Beam Steering", http://wwwrsphysse.anu.edu.au/~ggb112/publications/APL_paper.pdf, last accessed August 2005

11. Borg G.G., Harris J.H., Miljak D.G., Martin N.M., "Application of plasma Columns to Radiofrequency Antennas", Applied Physics Letters, Vol. 74, No. 22, pp.3272-3274, May 1999

12. Borg G.G., Harris J.H., Martin N.M., Thorncraft D., Milliken R., Miljak D.G., Kwan B., Ng T., Kircher J., "Plasmas as Antennas: Theory, Experiment and Applications", Physics of Plasmas, Vol. 7, No. 5, pp.2198-2202, May 2000

13. Dwyer T.J., Greig J.R., Murphy D.P., Perin J.M., Pechacek R.E., Raleigh M., "On the Feasibility of Using an Atmospheric Discharge Plasma as an RF Antenna", IEEE Transactions on Antennas and Propagation, Vol.AP-32, No. 2, pp. 141-146, February 1984

14. Liebermann, "Principles of Plasma Discharges and Material Processing", Chapters 6 and 14

15. Lorrain P., Corson D., "Electromagnetic Fields and Waves", 2nd Edition, pp. 481-492

16. Jenn D.C., "Plasma Antennas, Survey of Techniques and Current State of Art", NPS-CRC-03-001 (Report for Naval Postgraduate School)

17. Wort D.J.H., "The Emission of Microwave Noise by Plasma", Plasma Physics, vol. 4, pp. 353-357, 1962

18. Blatt Frank J., "Modern Physics", McGraw-Hill, 1992, Chapter 3

19. Davies K., "Ionospheric Radio Propagation", pp. 63-83, Dower Publication, Inc., New York, 1966

20. Oltman H. G., Huebner D. A., "Electromagnetically Coupled Microstrip Dipoles", IEEE Trans. Antennas and Propagation, Vol. AP-29, No. 1, pp. 151-157, January 1981

21. Das N. K., Pozar D. M., "Analysis and Design of Series-Fed Arrays of Printed Dipoles Proximity-Coupled to a Perpendicular Microstripline", IEEE Trans. Antennas and Propagation, Vol. 37, No. 4, pp.435-444, April 1989

22. Yang Hung-Yu, Alexopoulos N. G., Lepeltier P. M., Stern G. J., "Design of Transversely Fed EMC Microstrip Dipole Arrays Including Mutual Coupling", IEEE Trans. Antennas and Propagation, Vol. 38, No. 2, pp.145-151, February 1990

23. Tulinsef A. N., "Series-Fed-Type Linear Arrays of Dipole and Slot Elements Transversely Coupled to a Microstrip Line", Antennas and Propagation Society International Symposium, 1993. AP-S. Digest, Vol.1, pp. 128-131

24. G. Kumar, K. P. Ray, "Broadband Microstrip Antennas", Artech House, 2003

25. James J. R., Hall P. S., Wood C., "Microstrip Antenna Theory and Design", IEE Electromagnetic Wave Series 12, Peter Peregrinus Ltd., 1981

26. Jonscher A. K.; "Solid State Plasma Phenomena", Brit. J. Appl. Phys., Vol. 15, pp.365-377, 1964

27. Streetman Ben G.; "Solid State Electronic Devices", Prentice Hall, 4th Edition

28. Ioffe Physico-Technical Institute, http://www.ioffe.ru/SVA/NSM/Semicond, last accessed August 2005